

See discussions, stats, and author profiles for this publication at: <https://www.researchgate.net/publication/51724493>

# Rapid C–H Bond Activation by a Monocopper(III)–Hydroxide Complex

ARTICLE *in* JOURNAL OF THE AMERICAN CHEMICAL SOCIETY · NOVEMBER 2011

Impact Factor: 12.11 · DOI: 10.1021/ja207882h · Source: PubMed

---

CITATIONS

46

READS

93

## 6 AUTHORS, INCLUDING:



[Christopher J Cramer](#)

University of Minnesota Twin Cities

531 PUBLICATIONS 23,142 CITATIONS

[SEE PROFILE](#)



[Ritimukta Sarangi](#)

Stanford University

55 PUBLICATIONS 1,364 CITATIONS

[SEE PROFILE](#)

# Rapid C-H Bond Activation by a Monocopper(III)-Hydroxide Complex

Patrick J. Donoghue,<sup>1</sup> Jacqui Tehranchi,<sup>1</sup> Christopher J. Cramer,<sup>1</sup> Ritimukta Sarangi,<sup>2</sup> Edward I. Solomon,<sup>2,3</sup> and William B. Tolman<sup>1,\*</sup>

<sup>1</sup>Department of Chemistry, Center for Metals in Biocatalysis, and Supercomputer Institute, University of Minnesota, 207 Pleasant St. SE, Minneapolis, MN 55455 <sup>2</sup>Stanford Synchrotron Radiation Lightsource, SLAC National Accelerator Laboratory, Menlo Park, CA 94025 <sup>3</sup>Department of Chemistry, Stanford University, Stanford, CA 94305.

Supporting Information Placeholder

**ABSTRACT:** One electron oxidation of the tetragonal Cu(II) complex  $[\text{Bu}_4\text{N}][\text{LCuOH}]$  at  $-80^\circ\text{C}$  generated the reactive intermediate LCuOH, which was shown to be a Cu(III) complex on the basis of spectroscopy and theory ( $\text{L} = N,N'$ -bis(2,6-diisopropylphenyl)-2,6-pyridinedicarboxamide). The complex LCuOH reacts with dihydroanthracene to yield anthracene and the Cu(II) complex LCu(OH<sub>2</sub>). Kinetic studies showed that the reaction occurs via H-atom abstraction via a second-order rate law at high rates (cf.  $k = 1.1(1) \text{ M}^{-1}\text{s}^{-1}$  at  $-80^\circ\text{C}$ ,  $\Delta H^\ddagger = 5.4(2) \text{ kcal mol}^{-1}$ ,  $\Delta S^\ddagger = -30(2) \text{ eu}$ ) and with very large kinetic isotope effects (cf.  $k_{\text{H}}/k_{\text{D}} = 44$  at  $-70^\circ\text{C}$ ). The findings suggest that a Cu(III)-OH moiety is a viable reactant in oxidation catalysis.

Copper-oxygen species are implicated as intermediates in a wide range of oxidation reactions promoted by metalloenzymes,<sup>1</sup> synthetic complexes,<sup>2,3</sup> and materials.<sup>4</sup> Understanding the structures, properties, and reactivities of such species is critical for obtaining mechanistic insights into oxidation catalysis and for developing new, selective catalytic reagents and processes. Efforts to isolate and characterize reactive copper-oxygen intermediates through studies of copper-containing enzymes and synthetic model complexes have led to the identification of several core motifs,<sup>5</sup> exemplified by those shown in Chart 1. Complexes comprising cores **A-E** have been well-defined, and as a result have often been considered as viable oxidants in various catalytic reactions.<sup>6</sup> The monocopper-oxo/oxy core (**F**) has also been discussed<sup>7</sup> as a candidate capable of attacking hydrocarbon substrates (cf. by peptidylglycine  $\alpha$ -hydroxylating monooxygenase<sup>8</sup>) but examples of such species have only been characterized in the gas phase<sup>9</sup> and through theoretical calculations.<sup>8,10</sup> We report herein the preparation and character-

ization by spectroscopy and theory of a new type of copper-oxygen intermediate containing a hydroxo-copper(III) core (**G**), which formally may be considered as a protonated version of **F**.<sup>11</sup> The complex comprising **G** rapidly abstracts hydrogen atoms from the C-H bonds of dihydroanthracene, thus providing key precedent for the possible involvement of **G** in oxidation catalysis.

As starting material we used the tetragonal copper(II) complex LCu(CH<sub>3</sub>CN) (**1**,  $\text{L} = N,N'$ -bis(2,6-diisopropylphenyl)-2,6-pyridinedicarboxamide, Figure 1), for which we report a new X-ray crystal structure (Figure S1). Treatment of **1** suspended in Et<sub>2</sub>O or dissolved in THF with a solution of Bu<sub>4</sub>NX (X = Cl or OH) in MeOH yielded deep blue or green  $[\text{Bu}_4\text{N}][\text{LCuX}]$  ( $[\text{Bu}_4\text{N}][\mathbf{2}]$  or  $[\text{Bu}_4\text{N}][\mathbf{3}]$ ), respectively. Both products were isolated as solids and characterized by UV-vis, FTIR, and EPR spectroscopy, and CHN analysis.<sup>12</sup> Notable data include a sharp  $\nu(\text{OH})$  at  $3628 \text{ cm}^{-1}$  in the FTIR spectrum (nujol) of  $[\text{Bu}_4\text{N}][\mathbf{3}]$  and essentially axial EPR signals for both complexes consistent with tetragonal Cu(II) species (Figures S2-S3 and Table S1 in the Supporting Information). Crystals of both complexes suitable for characterization by X-ray diffraction were obtained by metathesis with PPNCl (Figures 1 and

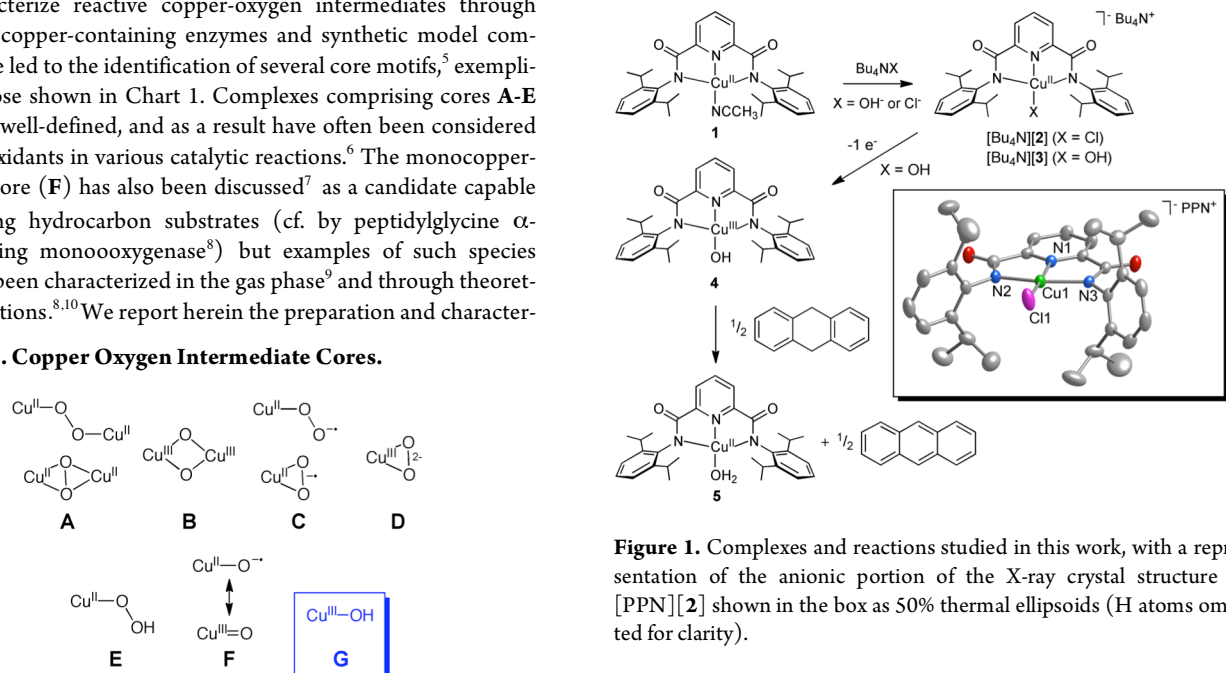


**Figure 1.** Complexes and reactions studied in this work, with a representation of the anionic portion of the X-ray crystal structure of  $[\text{PPN}][\mathbf{2}]$  shown in the box as 50% thermal ellipsoids (H atoms omitted for clarity).

S4, Table 1). While the structure of  $[PPN][\mathbf{2}]$  is straightforward, in  $[PPN][\mathbf{3}]$  the longer than expected Cu-O distance of 1.947(2) Å<sup>13</sup> led us to suspect that the crystals were a compositionally disordered<sup>14</sup> mixture of the chloride and hydroxide complexes, with the chloride ligand having been derived from displacement of hydroxide by the added PPNCl. Consistent with this notion, the UV-vis spectral features for  $[Bu_4N][\mathbf{3}]$  in THF cleanly converted to those for  $[Bu_4N][\mathbf{2}]$  upon addition of  $Bu_4NCl$  (1 equiv. from titration experiments; Figure S5). In addition, comparison of UV-vis spectra of crystals of  $[PPN][\mathbf{3}]$  (3 batches) to those of pure  $[Bu_4N][\mathbf{2}]$  and  $[Bu_4N][\mathbf{3}]$  indicated chloride contamination levels of 22–28%. Finally, DFT (*mPW*) calculations were performed for  $\mathbf{2}^-$  and  $\mathbf{3}^-$  that yielded minimum energy structures with Cu-N bond distances somewhat longer than those measured by X-ray crystallography (Table 1), as is common for *mPW* calculations with bulky ligands.<sup>15</sup> However, a significantly shorter Cu-OH distance was calculated for  $\mathbf{3}^-$  (1.863 Å) than was observed in the X-ray crystal structure (1.9465(19) Å). EXAFS data collected for  $[Bu_4N][\mathbf{3}]$  (powder, not exposed to PPNCl) were best fit with 4N/O donors<sup>16</sup> and average metal-ligand distances of 1.95 Å (Figures S6 and S7), slightly shorter than those determined by X-ray crystallography and *mPW* (Table 1). The EXAFS data collected for  $[Bu_4N][\mathbf{2}]$  were best fit with 3 N/O donors averaging 1.98 Å and one Cl donor at 2.21 Å, which is also in good agreement with the X-ray crystal structure and *mPW* calculations. Taken together, the data support the hypothesis of a compositionally disordered X-ray crystal structure for  $[PPN][\mathbf{3}]$  with a Cu-O distance that is overestimated by ~0.1 Å.

**Table 1. Selected Interatomic Distances for  $\mathbf{2}^-$  and  $\mathbf{3}^-$  from X-ray Crystallography and *mPW* Calculations<sup>a</sup>**

|                   | $\mathbf{2}^-$ |            | $\mathbf{3}^-$ |            |
|-------------------|----------------|------------|----------------|------------|
|                   | X-ray          | <i>mPW</i> | X-ray          | <i>mPW</i> |
| Cu-N1             | 1.926(2)       | 1.961      | 1.920(2)       | 1.947      |
| Cu-N2             | 1.992(2)       | 2.073      | 1.996(2)       | 2.078      |
| Cu-N3             | 1.993(2)       | 2.073      | 2.010(2)       | 2.080      |
| Cu-X <sup>b</sup> | 2.1842(8)      | 2.216      | 1.9465(19)     | 1.863      |
| Cu-N/O<br>(avg)   | 1.97           | 2.04       | 1.97           | 1.99       |

<sup>a</sup> Distances in Å; X-ray data for PPN<sup>+</sup> salts. <sup>b</sup> For  $\mathbf{2}^-$ , X = Cl; for  $\mathbf{3}^-$ , X = OH.

The tetragonal Cu(II) complex  $[Bu_4N][\mathbf{3}]$  exhibits a pseudoreversible oxidation in acetone solution (0.1 M  $Bu_4NPF_6$ ) at room temperature with  $E_{1/2}(\mathbf{3}^-) = -0.076$  V vs. Fc<sup>+/Fc</sup> (Figure S11). Chemical oxidation of  $[Bu_4N][\mathbf{3}]$  in acetone was performed using Fc<sup>+</sup>PF<sub>6</sub><sup>-</sup> at -80 °C,<sup>17</sup> which provided a deeply colored purple solution characterized by an intense low energy electronic absorption feature with  $\lambda_{max}$  ( $\epsilon$ ) = 540 nm (~12400 M<sup>-1</sup> cm<sup>-1</sup>) (Figure 2). The solutions were EPR silent. The absorption features decayed within minutes upon warming to -60 °C. Titration experiments monitored by UV-vis spectroscopy (Figure S12) showed that the oxidation reaction required 1 equivalent of oxidant to reach completion. Reduction of this species with 1 equivalent of decamethylferrocene (Fc<sup>\*</sup>) to the chilled solution yielded UV-vis features consistent with  $\mathbf{3}$  and Fc<sup>\*\*</sup> (Figures S13). These data are consistent

with a reversible 1-electron process that generates LCuOH (**4**, Figure 1).

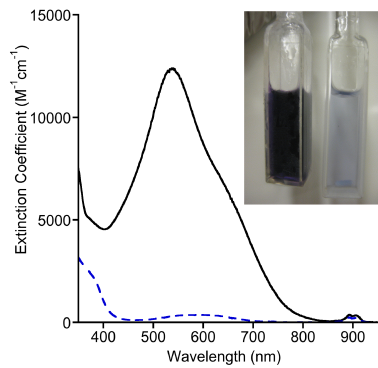


**Figure 2.** UV-vis spectra of  $[Bu_4N][\mathbf{3}]$  (blue dashed line, right cuvette in photograph) and **4** (solid black line, left cuvette in photograph) in acetone at -80 °C.

**Table 2. Selected Structural Parameters for **4** from *mPW* Calculations<sup>a</sup>**

|              | <i>singlet</i> | <i>triplet</i> |
|--------------|----------------|----------------|
| Cu-N1        | 1.888          | 1.960          |
| Cu-N2        | 1.992          | 2.074          |
| Cu-N3        | 1.992          | 2.074          |
| Cu-O         | 2.155          | 2.213          |
| Cu-N/O (avg) | 1.96           | 2.04           |

<sup>a</sup> All distances in Å.

Lacking crystals suitable for X-ray crystallography, we turned to DFT calculations and X-ray absorption spectroscopy to further evaluate the nature of **4**. The one electron oxidation of  $\mathbf{3}^-$  could conceivably result in (a) a metal based oxidation to yield a Cu(III) species, or (b) a ligand-based oxidation to yield a Cu(II)-ligand radical. A Cu(III) species should be a singlet whereas a Cu(II)-ligand radical could either be a triplet or an open-shell singlet. Starting from optimized *mPW* structures of  $\mathbf{3}^-$ , a closed shell singlet structure for **4** was located easily. This oxidized singlet maintained the square-planar geometry and symmetry elements identified in its Cu(II) precursor (*C*). Consistent with the singlet Cu(III) formulation, and in agreement with EXAFS results (see below), upon oxidation of  $\mathbf{3}^-$  to **4** the copper-ligand bonds contract; the average Cu-N bond shortens by 0.08 Å and the Cu-N/O bond average shortened by 0.09 Å (Table 2). Finally, the results of gas phase time dependent DFT (TD B98) calculations for the singlet of **4** match well with the experimentally observed UV-vis features (Figure S14). Thus, the singlet wavefunction for **4** was calculated to have a single transition at 589 nm (2.10 eV), within 0.2 eV of the observed transition at 540 nm (2.30 eV). The dominant one-electron excitation in this transition, with a weight of about 67%, is from an orbital with largely ligand (L)  $\pi$  character to one largely comprised of the Cu d<sub>2,γ,2</sub> (Figure S15). In sum, calculations support a singlet Cu(III) formulation for **4**.

Consistent with this conclusion, structures corresponding to a ligand based oxidation were more difficult to locate by *mPW*. Thus,

attempts to identify an open-shell singlet via a broken-symmetry formalism for **4** converged to closed-shell singlet solutions. A triplet structure can be located, but is energetically disfavored relative to the closed-shell singlet by 19.0 kcal/mol. Metal-ligand bond distances calculated for the triplet also are relatively unchanged relative to those calculated for the precursor **3**<sup>-</sup>, in contrast to the EXAFS results (see below). Thus, the triplet **4** actually has a slightly longer average Cu-N/O bond length than the starting complex **3**<sup>-</sup> (2.01 Å vs 1.99 Å). Finally, TD B98 results for the triplet included several transitions in the near-IR range that were not observed experimentally.

Cu K-edge XAS data provide direct experimental evidence for the Cu(III) formulation of **4**. As shown in Figure 3, the Cu K pre-edge energy position of **4** is shifted ~1.7 eV to higher energy relative to pre-edge of the Cu(II) complex [Bu<sub>4</sub>N][**3**], indicating one electron metal based oxidation with an associated increase in ligand field strength of the Cu center. A shift in the rising edge by ~1.1 eV is also observed on going from [Bu<sub>4</sub>N][**3**] to **4** reflecting the increase in the effective nuclear charge on Cu in **4**.<sup>18</sup> The EXAFS data (Figures S6 and S8 and Table S3) provide further confirmation of the Cu(III) nature of **4**. Fits to the data show an ~0.1 Å shortening of the first shell Cu-O/N bond distances in **4** (4 Cu-N/O at 1.86 Å) relative to [Bu<sub>4</sub>N][**3**] (4 Cu-N/O at 1.95 Å), typical for oxidation of a Cu(II) to a Cu(III) complex.

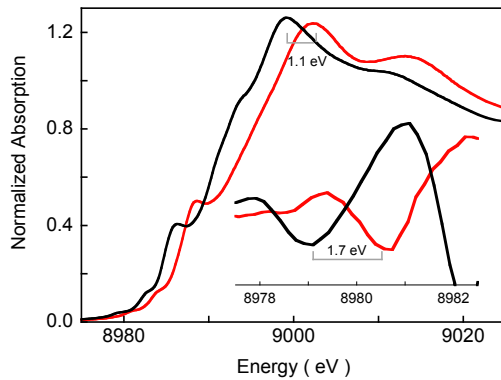


**Figure 3.** The normalized Cu K-edge XAS spectra of [Bu<sub>4</sub>N][**3**] (—) and **4** (—). The inset shows the second derivative spectra of the pre-edge region showing the shift on going from [Bu<sub>4</sub>N][**3**] and **4**.

Inspired by reports of C-H bond activation by Mn(III), Mn(IV), and Fe(III) hydroxide complexes,<sup>19</sup> we examined the reactivity of **4** with dihydroanthracene (DHA), a commonly studied substrate useful for comparison purposes. The UV-vis features of **4** smoothly decayed upon introduction of 0.5 equiv DHA to acetone solutions at low temperature, concomitant with the growth of bands due to the formation of anthracene (85% yield by GC/MS). The final inorganic product was determined to be the Cu(II) complex LCu(OH)<sub>2</sub> (**5**, Figure 1) on the basis of comparison of the UV-vis spectrum to that of independently synthesized material, which was fully characterized, including by X-ray crystallography (Figure S16). The UV-vis features of **4** decayed according to pseudo-first-order kinetics when the reaction was performed with excess DHA (10-40 equiv), and a plot of  $k_{\text{obs}}$  vs. [DHA] was linear with an intercept that corresponded to the self decay rate (Figures S17 and S18). These data indicate an overall second-order rate law  $-d[\mathbf{4}]/dt = k[\mathbf{4}][\text{DHA}]$ . A very large kinetic isotope effect ( $k_{\text{H}}/k_{\text{D}}$ ) of 44 at -70 °C was observed when the reaction was performed

with DHA-*d*<sub>4</sub>, and the temperature dependence of this effect was evaluated by an Eyring analysis (Figure 4, Table S4);  $\Delta H^{\ddagger}_{\text{H}} = 5.4(2)$  kcal mol<sup>-1</sup>,  $\Delta S^{\ddagger}_{\text{H}} = -30(2)$  eu,  $\Delta H^{\ddagger}_{\text{D}} = 6.2(3)$  kcal mol<sup>-1</sup>,  $\Delta S^{\ddagger}_{\text{D}} = -34(3)$  eu. Based on these parameters, the KIE was calculated to be 29 at 20 °C, well beyond the semiclassical limit. Finally, we note that **4** reacted essentially instantaneously at -80 °C with 2,4,6-tri-*tert*-butylphenol to yield the phenoxyl radical (UV-vis, EPR). Together, the reactivity and kinetic data support a mechanism for oxidation of DHA to anthracene that involves rate-determining H-atom abstraction by the Cu(III)-OH moiety, with a tunneling contribution being a reasonable rationale for the larger than semiclassically predicted  $k_{\text{H}}/k_{\text{D}}$  values.

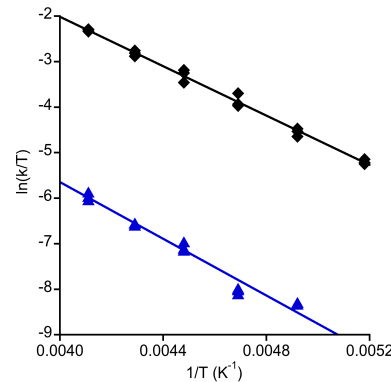


**Figure 4.** Plots of  $\ln(k/T)$  vs.  $1/T$  (where  $k$  = second order rate constant,  $T$  = temperature in K) for the reaction of **4** with DHA (black diamonds) or DHA-*d*<sub>4</sub> (blue triangles). The shown linear fits were used to calculate the activation parameters listed in the text via the Eyring equation ( $R = 0.997$  and  $0.985$ , respectively).

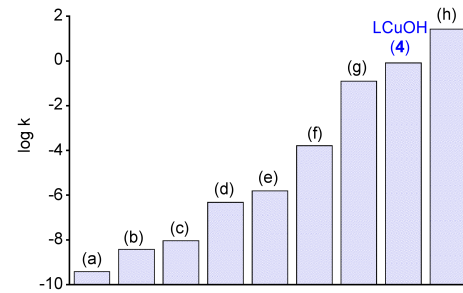


**Figure 5.** Comparison of the second order rate constants ( $k$  in units of  $\text{M}^{-1}\text{s}^{-1}$ , on a logarithmic scale) for oxidation of DHA at -80 °C by selected copper, iron, and manganese complexes with that of LCuOH (**4**). For (g) and (h), reported rate constants were used; for (a)-(f), the rate constants were calculated using the Eyring equation from the reported activation parameters. (a)  $[\text{Cu}^{\text{III}}(\text{Pre})]^+$  (ref. 20) (b)  $[\text{Fe}^{\text{III}}(\text{H}_2\text{bim})_2]^{2+}$  (ref. 21), (c)  $[\text{Fe}^{\text{III}}(\text{PYS})\text{OH}]^{2+}$  (ref. 22), (d)  $[\text{Mn}^{\text{III}}(\text{H}_3\text{buea})\text{O}]$ ,  $[\text{MnO}_4]$  (refs. 23, 24) (e)  $[\text{Mn}^{\text{III}}(\text{PY5})\text{OH}]^{2+}$  (ref. 25), (f)  $[\text{Mn}^{\text{IV}}(\text{H}_3\text{buea})\text{O}]$ , (ref. 23) (g)  $[\text{L}'(\text{CH}_3\text{CN})\text{Fe}^{\text{IV}}\text{O}]^{2+}$  (ref. 26), and (h)  $[\text{L}'\text{Fe}^{\text{III}}(\text{OH})(\mu\text{-O})(\text{L}')\text{Fe}^{\text{IV}}\text{O}]^{2+}$  (ref. 26). Abbreviations: Pre = 3,9-dimethyl-4,8-diazaundecane-2,10-dionedioximate H<sub>2</sub>bim = 2,2'-bi-imidazoline, PY5 = 2,6-bis(bis(2-pyridyl)methoxy-methane)pyridine, H<sub>3</sub>buea<sup>3-</sup> = triply deprotonated form of tris[(*N*'-*tert*-butylureayl)-*N*-ethylene]amine, L' = tris((4-methoxy-3,5-di-methylpyridin-2-yl)methyl)amine).

The second-order rate constants for reactions of selected relevant Cu(III) or metal-oxo or -hydroxo complexes with DHA at -80 °C are compared to that of **4** in Figure 5.<sup>20-26</sup> The rate of H-atom ab-

straction from DHA by LCuOH is significantly faster than most other nonheme iron (b,c,g), manganese (d-f), and copper (a) reagents and is comparable to a recently reported high-spin Fe(III)Fe(IV)-oxo complex (h). While not as intrinsically reactive as the ( $P^+$ )Fe(IV)=O intermediate (compound 1) in cytochrome P450,<sup>27</sup> the high rate for DHA oxidation by 4 is nonetheless extraordinary in the context of known oxidizing capabilities of copper-oxygen species.<sup>5,7,28</sup> While further work is necessary to understand the basis for this reactivity, we speculate that high basicity of the hydroxide group is a key factor in view of the fact that the potential for  $3^-/4$  couple is modest ( $-0.076$  V vs.  $Fc^+/Fc$ ).<sup>29</sup> Similar arguments have been advanced to rationalize observed rates of H-atom transfer by Mn(V)-oxo<sup>30</sup> and Fe(IV)-imido<sup>31</sup> complexes, as well as cuprous oxide surfaces.<sup>32</sup> The relatively minor structural differences (overall geometry, metal-ligand bond distances) between 4 and 5 may also result in a small reorganization energy that could contribute to a high reaction rate.<sup>33</sup>

In summary, we have prepared a new type of copper-oxygen intermediate and shown through theory and experiment that it is best described as a singlet Cu(III)-OH complex. High rates of H-atom abstraction from phenols and DHA by this complex were observed, indicating that such a species should be considered as a viable intermediate in catalytic oxidation reactions.

## ASSOCIATED CONTENT

**Supporting Information.** Experimental details, including characterization data, spectra, X-ray structure drawings, kinetic plots and tables, and calculation protocols and results (PDF) and CIFs. This material is available free of charge via the Internet at <http://pubs.acs.org>.

## AUTHOR INFORMATION

### Corresponding Author

wtolman@umn.edu

### ACKNOWLEDGMENT

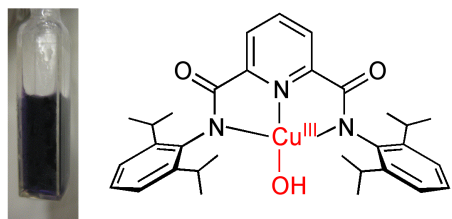
This research was supported by the NIH (grants R37-GM47365 to W. B. T.; DK-31450 to E. I. S.) and the NSF (CHE-0952054 to CJC). SSRL operations are funded by the Department of Energy, Office of Basic Energy Sciences. The SSRL Structural Molecular Biology program is supported by the National Institutes of Health, National Center for Research Resources, Biomedical Technology Program, and the Department of Energy, Office of Biological and Environmental Research. This publication was made possible by Award P41 RR001209 from the National Center for Research Resources (NCRR), a component of the National Institutes of Health (NIH).

## REFERENCES

- (1) Klinman, J. P. *Chem. Rev.* **1996**, *96*, 2541-2561. Solomon, E. I.; Sundaram, U. M.; Machonkin, T. E. *Chem. Rev.* **1996**, *96*, 2563-2605.
- (2) Diaz-Requejo, M. M.; Perez, P. J. *Chem. Rev.* **2008**, *108*, 3379-3394.
- (3) Que, L., Jr.; Tolman, W. B. *Nature* **2008**, *455*, 333-340.
- (4) Woertink, J. S.; Smeets, P. J.; Groothaert, M. H.; Vance, M. A.; Sels, B. F.; Schoonheydt, R. A.; Solomon, E. I. *Proc. Natl. Acad. Sci. USA* **2009**, *106*, 18908-18913.
- (5) Lewis, E. A.; Tolman, W. B. *Chem. Rev.* **2004**, *104*, 1047-1076. Mirica, L. M.; Ottenwaelder, X.; Stack, T. D. P. *Chem. Rev.* **2004**, *104*, 1013-1045. Hatcher, L.; Karlin, K. D. *J. Biol. Inorg. Chem.* **2004**, *9*, 669-683. Itoh, S. *Curr. Opin. Chem. Biol.* **2006**, *10*, 115-122.
- (6) For example, see: Itoh, S.; Fukuzumi, S. *Acc. Chem. Res.* **2007**, *40*, 592-600.
- (7) Himes, R. A.; Karlin, K. D. *Curr. Opin. Chem. Biol.* **2009**, *13*, 119-131. Hong, S.; Gupta, A. K.; Tolman, W. B. *Inorg. Chem.* **2009**, *48*, 6323-6325 and references cited therein.
- (8) Chen, P.; Solomon, E. I. *J. Am. Chem. Soc.* **2004**, *126*, 4991-5000. Evans, J. P.; Ahn, K.; Klinman, J. P. *J. Biol. Chem.* **2003**, *278*, 49691-49698. Yoshizawa, K.; Kihara, N.; Kamachi, T.; Shiota, Y. *Inorg. Chem.* **2006**, *45*, 3034-3041. Crespo, A.; Marti, M. A.; Roitberg, A. E.; Amzel, L. M.; Estrin, D. A. *J. Am. Chem. Soc.* **2006**, *128*, 12817-12828.
- (9) Schröder, D.; Holthausen, M. C.; Schwarz, H. *J. Phys. Chem. B* **2004**, *108*, 14407-14416. Dietl, N.; van der Linde, C.; Schlangen, M.; Beyer, M. K.; Schwarz, H. *Angew. Chem. Int. Ed.* **2011**, *50*, 4966-4969.
- (10) Yoshihide, N.; Kimihiko, H.; Tetsuya, T. *J. Chem. Phys.* **2001**, *114*, 7935-7940. Decker, A.; Solomon, E. I. *Curr. Opin. Chem. Biol.* **2005**, *9*, 152-163. Gherman, B. F.; Heppner, D. E.; Tolman, W. B.; Cramer, C. J. *J. Biol. Inorg. Chem.* **2006**, *11*, 197-205. Huber, S. M.; Ertem, M. Z.; Aquilante, F.; Gagliardi, L.; Tolman, W. B.; Cramer, C. J. *Chem. Eur. J.* **2009**, *15*, 4886-4895. Gherman, B. F.; Tolman, W. B.; Cramer, C. J. *J. Comp. Chem.* **2006**, *27*, 1950-1961.
- (11) Protonation of a species with core F to yield a compound with core G has been postulated: Reinaud, O.; Capdevielle, P.; Maumy, M. *J. Chem. Soc., Chem. Commun.* **1990**, 566-568.
- (12) See the supporting information.
- (13) Some reported Cu-OH bond distances in terminal monocuppper-hydroxide complexes: 1.878(2) Å, Berreau, L. M.; Mahapatra, S.; Halfen, J. A.; Young, V. G., Jr.; Tolman, W. B. *Inorg. Chem.* **1996**, *35*, 6339-6342. 1.875(2) Å, Lee, S. C.; Holm, R. H. *J. Am. Chem. Soc.* **1993**, *115*, 11789-1198.
- (14) Parkin, G. *Chem. Rev.* **1993**, *93*, 887-911.
- (15) Cramer, C. J. "Essentials of Computational Chemistry: Theories and Models", 2nd ed.; Wiley & Sons: New York, 2004. p 291.
- (16) Large Debye-Waller factors for this fit are consistent with a spread of Cu-N/O distances, consistent with the X-ray data and DFT calculations.
- (17) XAS samples were prepared using  $(p\text{-tolyl})_3N^+PF_6^-$ .
- (18) DuBois, J. L.; Mukherjee, P.; Stack, T. D. P.; Hedman, B.; Solomon, E. I.; Hodgson, K. O. *J. Am. Chem. Soc.* **2000**, *122*, 5775-5787.
- (19) Shi, S.; Wang, Y.; Xu, A.; Wang, H.; Zhu, D.; Roy, S. B.; Jackson, T. A.; Busch, D. H.; Yin, G. *Angew. Chem. Int. Ed.* **2011**, *50*, 7321-7324, and references cited therein.
- (20) Lockwood, M. A.; Blubaugh, T. J.; Collier, A. M.; Lovell, S.; Mayer, J. M. *Angew. Chem. Int. Ed.* **1999**, *38*, 225-227.
- (21) Roth, J. P.; Mayer, J. M. *Inorg. Chem.* **1999**, *38*, 2760-2761.
- (22) Goldsmith, C. R.; Stack, T. D. P. *Inorg. Chem.* **2006**, *45*, 6048-6055.
- (23) Parsell, T.; Yang, M.; Borovik, A. *J. Am. Chem. Soc.* **2009**, *131*, 2762-2763.
- (24) Gardner, K. A.; Kuehnert, L. L.; Mayer, J. M. *Inorg. Chem.* **1997**, *36*, 2069-2078.
- (25) Goldsmith, C. R.; Cole, A. P.; Stack, T. D. P. *J. Am. Chem. Soc.* **2005**, *127*, 9904-9912.
- (26) Xue, G.; De Hont, R.; Münck, E.; Que, L., Jr. *Nature Chemistry* **2010**, *2*, 400-405.
- (27) Rittle, J.; Green, M. T. *Science* **2010**, *330*, 933-937.
- (28) Itoh, S. *Curr. Opin. Chem. Biol.* **2006**, *10*, 115-122.
- (29) Green, M. T. *Curr. Opin. Chem. Biol.* **2009**, *13*, 84-88.
- (30) Prokop, K. A.; de Visser, S. P.; Goldberg, D. P. *Angew. Chem. Int. Ed.* **2010**, *49*, 5091-5095.
- (31) Nieto, I.; Ding, F.; Bontchev, R. P.; Wang, H.; Smith, J. M. *J. Am. Chem. Soc.* **2008**, *130*, 2716-2717.
- (32) Reitz, J. B.; Solomon, E. I. *J. Am. Chem. Soc.* **1998**, *120*, 11467-11478.
- (33) Mayer, J. M. *Acc. Chem. Res.* **2011**, *44*, 36-46.

Table of Contents graphic:

---



**Supporting Information**  
**For**

***Rapid C-H Bond Activation by a Monocopper(III)-Hydroxide Complex***

Patrick J. Donoghue,<sup>1</sup> Jacqui Tehranchi,<sup>1</sup> Christopher J. Cramer,<sup>1</sup> Ritimukta Sarangi,<sup>2</sup> Edward I. Solomon,<sup>2,3</sup> and William B. Tolman<sup>1,\*</sup>

<sup>1</sup>Department of Chemistry, Center for Metals in Biocatalysis, and Supercomputer Institute, University of Minnesota, 207 Pleasant St. SE, Minneapolis, MN 55455 <sup>2</sup>Stanford Synchrotron Radiation Lightsource, SLAC National Accelerator Laboratory, Menlo Park, CA 94025 <sup>3</sup>Department of Chemistry, Stanford University, Stanford, CA 94305.

## Experimental Details

**General.** All chemicals were purchased from Aldrich and used without purification unless listed below. Spectroscopic grade acetone was degassed and dried over activated 3 Å molecule sieves for a minimum of two days then distilled under vacuum. Purified acetone was stored in a nitrogen filled glove box and filtered through a 0.45 µm PTFE syringe filter immediately before use. Dihydroanthracene was recrystallized from ethanol. *N,N'*-Bis(2,6-diisopropylphenyl)-2,6-pyridinedicarboxamide<sup>1</sup>, tris(p-tolyl)ammonium hexafluorophosphate ((p-tolyl)<sub>3</sub>NPF<sub>6</sub>)<sup>2</sup>, and d<sub>4</sub>-dihydroanthracene<sup>3</sup> were prepared as previously described.

**Physical methods.** UV-vis spectra were collected on a HP8453 (190-1000 nm) diode array spectrophotometer. Low temperature UV-vis experiments were performed using a Unisoku low temperature UV-vis cell holder. In the event of minimal frosting in the low temperature cell holder, baseline corrections were performed by subtracting an average region of no absorbance from the spectra (950-980 nm). GC-MS analysis was performed using an Agilent Technologies 7890A GC system and 5975C VL MSD. Elemental analyses were performed by Robertson Microlit Laboratory (Ledgewood, NJ). Infrared spectra were collected on a Nicolet Avatar 370 FT-IR equipped with a Smart OMNI Sampler. EPR data was collected on a Bruker Elexsys E500 spectrometer using X-band radiation at 2 K. Simulations were performed using Bruker SimFonia software (version 1.25).

**X-ray Absorption Spectroscopy.** The Cu K-edge X-ray absorption spectra of [Bu<sub>4</sub>N][2], [Bu<sub>4</sub>N][3], and 4 were measured at the Stanford Synchrotron Radiation Lightsource (SSRL) on the 20 pole, 2 T wiggler beamline 7-3 under standard ring conditions of 3 GeV and ~300 mA ring current. A Si(220) double-crystal monochromator was used for energy selection. Other optical components used for the experiments were a cylindrical Rh-coated bent focusing mirror. Spectra were collected in the fully tuned configuration of the monochromator. The solution samples were immediately frozen after preparation and stored under liquid N<sub>2</sub> until measurement. During data collection, the samples were maintained at a constant temperature of ~10 K using an Oxford Instruments CF 1208 liquid helium cryostat. Data were measured to  $k=14 \text{ \AA}^{-1}$  by using a Canberra Ge 30-element array detector. Internal energy calibration was accomplished by simultaneous measurement of the absorption of a Cu-foil placed between two ionization chambers situated after the sample. The first inflection point of the foil spectrum was fixed at 8980.3 eV. The samples were monitored for photoreduction and to minimize the effect of beam damage, a single spectrum was obtained from each sample spot. A total of 8 sample spots were exposed and the data presented here are 8 scan average spectra for all samples. The data were processed by fitting a second-order polynomial to the pre-edge region and subtracting this from the entire spectrum as background. A four-region spline of orders 2, 3, 3 and 3 was used to model the smoothly decaying post-edge region. The data were normalized by subtracting the cubic spline and assigning the edge jump to 1.0 at 9000 eV using the Pyspline program.<sup>4</sup> Theoretical EXAFS signals  $\chi(k)$  were calculated by using FEFF (Macintosh version 8.4)<sup>5-7</sup> and

(1) Wasilke, J.-C.; Wu, G.; Bu, X.; Kehr, G.; Erker, G. *Organometallics* **2005**, *24*, 4289.

(2) Manner, V. W.; DiPasquale, A. G.; Mayer, J. M. *J. Am. Chem. Soc.* **2008**, *130*, 7210.

(3) Goldsmith, C. R.; Jonas, R. T.; Stack, T. D. P. *J. Am. Chem. Soc.* **2002**, *124*, 83.

(4) Tenderholt, A. *Pyspline and QMForge*, 2007.

(5) Rehr, J. J.; Albers, R. C. *Rev. Mod. Phys.* **2000**, *72*, 621-654.

(6) Rehr, J. J.; Mustre de Leon, J.; Zabinsky, S. I.; Albers, R. C. *J. Am. Chem. Soc.* **1991**, *113*, 5135-5140.

(7) Mustre de Leon, J.; Rehr, J. J.; Zabinsky, S. I.; Albers, R. C. *Phys. Rev. B: Condens. Matter* **1991**, *44*, 4146-4156.

the crystal structure of [PPN][2] and [PPN]3 and a structural model of 4 made using Avogadro. The theoretical models were fit to the data using EXAFSPAK.<sup>8</sup> The structural parameters varied during the fitting process were the bond distance (R) and the bond variance  $\sigma^2$ , which is related to the Debye-Waller factor resulting from thermal motion, and static disorder of the absorbing and scattering atoms. The non-structural parameter  $E_0$  (the energy at which  $k=0$ ) was also allowed to vary but was restricted to a common value for every component in a given fit. Coordination numbers was systematically varied in the course of the fit but were fixed within a given fit.

**[N,N'-Bis(2,6-diisopropylphenyl)-2,6-pyridinedicarboxamido]acetonitrilecopper(II)**

**(LCu(CH<sub>3</sub>CN), 1):** The title compound was prepared using a modified procedure to the one previously described.<sup>9</sup> Into a 100 mL round bottom flask was placed bis(2,6-diisopropylphenyl)pyridine-2,6-dicarboxamide (0.487 g, 1.00 mmol) and copper(II) triflate (0.346 g, 0.96 mmol). The solids were dissolved in 50 mL of MeOH forming a pale green solution. Sodium methoxide (0.5 M in methanol, 4.00 mL, 2.00 mmol) was then added causing the solution to immediately turn deep green. The solution was stirred at room temperature for 10 min, after which the solvents were removed *in vacuo*. The dark green residue was dissolved in 50 mL CH<sub>3</sub>CN, forming a mahogany solution. The solvents were again removed *in vacuo* and the residue dissolved in 50 mL CH<sub>2</sub>Cl<sub>2</sub> and filtered to remove sodium triflate. The remaining solution was evaporated and the solids dissolved in a minimum of CH<sub>3</sub>CN (20 mL) diluted with toluene (80 mL) and placed in the freezer overnight whereupon dark mahogany crystals formed. The crystalline solid was isolated by filtration and dried *in vacuo* (0.446 g, 79.2%). Crystals suitable for X-ray diffraction were prepared by slow evaporation of an acetonitrile solution of the product at -30 °C to give deep red blocks. Analytical data matched previously reported values.<sup>9</sup>

**Tetrabutylammonium [N,N'-Bis(2,6-diisopropylphenyl)-2,6-pyridinedicarboxamido]copper(II) chloride ([Bu<sub>4</sub>N][LCuCl], [Bu<sub>4</sub>N][2]):** To a solution of 1 (147.9 mg, 0.25 mmol) in THF (15 mL) was added Bu<sub>4</sub>NCl (70.0 mg, 0.25 mmol). The solution was stirred at room temperature for 30 min during which time it turned deep green. The solvent was then removed *in vacuo*. The residual green solid was suspended in 15 mL of Et<sub>2</sub>O, stirred for 30 min and evaporated (3x) to help remove residual THF. The powdery solid was then suspended in 15 mL Et<sub>2</sub>O and allowed to stir overnight. The solution was then filtered, the collected solids were washed with an additional 10 mL Et<sub>2</sub>O, and then further dried *in vacuo* overnight to yield the product as a green powder (166.4 mg, 80.2%). Crystals suitable for X-ray diffraction were prepared by adding one equivalent of PPNCl to 1 in THF, followed by vapor diffusion of hexanes at -30 °C to yield bright green needles. UV-vis (acetone, -80 °C)  $\lambda_{\text{max}}$ , nm ( $\epsilon$ ): 400 (3330), 625 (432). Anal. Calcd for C<sub>47</sub>H<sub>73</sub>ClCuN<sub>4</sub>O<sub>2</sub>: C, 68.42; H, 8.92; N, 6.79; Cl, 4.30. Found: C, 68.31; H, 9.32; N, 6.63; Cl, 4.77.

**Tetrabutylammonium [N,N'-Bis(2,6-diisopropylphenyl)-2,6-pyridinedicarboxamido]copper(II) hydroxide ([Bu<sub>4</sub>N][LCuOH], [Bu<sub>4</sub>N][3]):** To a suspension of 1 (146.7 mg, 0.25 mmol), in Et<sub>2</sub>O (15 mL) was added 0.25 mL of Bu<sub>4</sub>NOH solution in MeOH (1.0 M, 0.25 mmol). A blue precipitate formed immediately. The solution was stirred at room temperature for 30 min, after which the solvents were removed *in vacuo*. The residual solids were suspended in 15 mL of Et<sub>2</sub>O, stirred for 30 min and evaporated (2x) to help remove any residual MeOH. The powdery solid was then suspended in 15 mL Et<sub>2</sub>O and allowed to stir overnight. The mixture was then

(8) George, G. N. *EXAFSPAK and EDG-FIT*, 2000.

(9) Donoghue, P. J.; Gupta, A. K.; Boyce, D. W.; Cramer, C. J.; Tolman, W. B. *J. Am. Chem. Soc.* **2010**, *132*, 15869.

filtered, the collected solids were washed with an additional 10 mL Et<sub>2</sub>O, and then further dried *in vacuo* overnight to yield the product as a blue powder (150.5 mg, 74.8%). Crystals suitable for X-ray diffraction were prepared by adding 1 equivalent of PPNCl to a solution of [Bu<sub>4</sub>N][3] in THF followed by vapor diffusion of hexanes at -30 °C to yield deep blue needles. UV (acetone, -80 °C)  $\lambda_{\text{max}}$ , nm ( $\epsilon$ ): 360 (sh, 2807), 592 (397). Anal. Calcd for C<sub>47</sub>H<sub>74</sub>CuN<sub>4</sub>O<sub>3</sub>: C, 69.98; H, 9.25; N, 6.95. Found: C, 69.23; H, 9.18; N, 6.83.

**[N,N'-Bis(2,6-diisopropylphenyl)-2,6-pyridinedicarboxamido]aquacopper(II)**

**(LCu(OH<sub>2</sub>), 5):** This complex was prepared via a procedure similar to that used for the synthesis of **1**. Into a 100 mL round bottom flask was placed bis(2,6-diisopropylphenyl)pyridine-2,6-dicarboxamide (0.4861 g, 1.00 mmol) and copper(II) triflate (0.3456 g, 0.96 mmol). The solids were dissolved in 50 mL of MeOH forming a pale green solution. Sodium methoxide (0.5 M in MeOH, 4.0 mL, 2.00 mmol) was then added causing the solution to immediately turn deep green. The solution was stirred at room temperature for 10 min, after which the solvents were removed *in vacuo*. The dark green residue was dissolved in 50 mL CH<sub>3</sub>CN, forming a mahogany solution. The solvent was again removed *in vacuo* and the residue dissolved in 50 mL CH<sub>2</sub>Cl<sub>2</sub> and filtered to remove sodium triflate. The solvent was evaporated and the solid residue was dissolved in 10 mL of acetone and 10 mL H<sub>2</sub>O. The solvents were evaporated, and the residue dissolved in 20 mL of the 1:1 acetone/water mixture twice more to ensure complete removal of CH<sub>3</sub>CN. The solvents were evaporated to yield a purple solid that was dried *in vacuo* to yield the product as a dark brown powder (0.4878 g, 86.3%). Crystals suitable for X-ray diffraction were prepared by the slow evaporation of an acetone solution of the brown powder at -30 °C to give brown needles. UV (acetone, -80 °C)  $\lambda_{\text{max}}$ , nm ( $\epsilon$ ): 398 (3067), 558 (692). Anal. Calcd for C<sub>31</sub>H<sub>39</sub>CuN<sub>3</sub>O<sub>3</sub>: C, 65.88; H, 6.95; N, 7.43. Found: C, 66.36; H, 6.80; N, 7.50.

**Procedure for the oxidation of [Bu<sub>4</sub>N][LCuOH], [Bu<sub>4</sub>N][3]:** All reactions involving chemical oxidants were performed either in a nitrogen filled glove box or in septum sealed Schlenk flasks under nitrogen or argon. For a typical reaction monitored by UV-vis spectroscopy, 3 mM stock solutions of [Bu<sub>4</sub>N][3] and ferrocenium hexafluorophosphate (FcPF<sub>6</sub>) were prepared in acetone. A 0.1 mL aliquot of the stock solution of [Bu<sub>4</sub>N][3] was added to a UV-vis cuvette along with 2.8 mL of acetone. After cooling the cuvette to -80 °C, 0.1 mL of the FcPF<sub>6</sub> solution was added, causing the immediate formation of an intensely purple species (note: after the addition of the oxidant, the cuvette held 3 mL of a solution that was 0.1 mM in Cu). For reactivity studies with DHA, fluorene or diphenylmethane, the appropriate amount of substrate (10 to 2000 equivalents) was added to the cuvette along with [Bu<sub>4</sub>N][3] prior to cooling to the appropriate temperatures or addition of the oxidant. EPR samples were prepared by injecting a 0.1 mL aliquot of a stock solution (2 mM) of [Bu<sub>4</sub>N][3] into a quartz EPR sample tube and cooling to -78 °C in a dry ice/acetone bath. A 0.1 mL aliquot of a FcPF<sub>6</sub> stock solution (2 mM) was then added. The solution was mixed using a cannula as a stir rod and then the sample was frozen in liquid nitrogen for storage and analysis. Samples for XAS analysis were prepared by adding 0.8 mL of a 12.5 mM solution of [Bu<sub>4</sub>N][3] to a Schlenk flask. The solution was cooled to -78 °C in a dry ice/acetone bath whereupon 0.2 mL of a 50 mM solution of (p-tolyl)<sub>3</sub>NPF<sub>6</sub> was added. An aliquot of this solution (0.3 mL) was then transferred to an XAS sample cell that was buried in dry ice via a syringe cooled in the dry ice/acetone bath. The sample was then immediately frozen in liquid nitrogen for analysis. (Note: The aminium oxidant was used for the XAS samples due to a complicating side reaction of the oxidized product prepared from FcPF<sub>6</sub> with CO<sub>2</sub> (under investigation). UV-vis spectroscopic data showed that the same intermediate formed regardless of the choice of oxidant used.

**Cu K-edge XAS and EXAFS Analysis of [Bu<sub>4</sub>N][3] and 4.** The normalized Cu K-edge XAS spectra of [Bu<sub>4</sub>N][3] and 4 are shown in the main manuscript (Figure 3). The weak pre-edge transition observed below the onset of the rising-edge occurs due to an electric dipole-forbidden quadrupole-allowed 1s→3d transition. The energy position of the pre-edge transition is dominantly affected by the strength of the ligand field, which reflects the  $Z_{eff}$  on the Cu center.<sup>10</sup> For a Cu(II) complex this transition typically occurs at ~8979 eV and is shifted up by ~2 eV for a Cu(III) complex (~8981 eV).<sup>11</sup> The pre-edge transition in [Bu<sub>4</sub>N][3] and 4 occur at 8979.1 eV and 8980.8 eV, respectively clearly showing a 1.7 eV shift on going from [Bu<sub>4</sub>N][3] to 4 (Table S2). For a given ligand system, the Cu K- rising-edge shifts to higher energy with oxidation state. The rising edge maximum for [Bu<sub>4</sub>N][3] and 4 occur at 8999.3 and 9000.4 eV, respectively, indicating a 1.1 eV shift on going from [Bu<sub>4</sub>N][3] to 4. The shift to higher energy observed in both the pre-edge and rising-edge region clearly indicate that [Bu<sub>4</sub>N][3] is a Cu(II) species whereas 4 is a one electron oxidized Cu(III) species.

A comparison of the  $k^3$  weighted Cu K-edge EXAFS for [Bu<sub>4</sub>N][3] and 4 along with their non-phase shift corrected Fourier transforms ( $k=2\text{-}13.2 \text{ \AA}^{-1}$ ) is shown in Figure S6. FEFF fits to the data are presented in Figures S7 and S8 and Table S3. On going from [Bu<sub>4</sub>N][3] to 4, the EXAFS beat pattern shifts to higher  $k$  and the first shell Fourier transform peak intensity increases and shifts to lower  $R'$ . This indicates a decrease in first shell bond distances in 4. FEFF fits reveal 4 Cu-N/O interactions at 1.95 Å in [Bu<sub>4</sub>N][3] and 4 Cu-N/O interactions at 1.86 Å in 4 (Table S3). The second and third shell for [Bu<sub>4</sub>N][3] and 4 were fit with single and multiple-scattering components from the nitrogenous ligand (see Table S3). The ~0.1 Å shortening of the first shell Cu-N/O distances is also consistent with the oxidation of Cu(II) in [Bu<sub>4</sub>N][3] to Cu(III) in 4.

**Cu K-edge XAS and EXAFS of [Bu<sub>4</sub>N][2] and [Bu<sub>4</sub>N][3].** Figure S9 shows a comparison of the Cu K-edge XAS spectra of [Bu<sub>4</sub>N][2] and [Bu<sub>4</sub>N][3]. The inset shows the second derivative of the pre-edge region. The pre-edge of both [Bu<sub>4</sub>N][2] and [Bu<sub>4</sub>N][3] occur at ~8979.1 eV indicating that both are Cu(II) complexes. The rising-edge spectra for the two complexes have an intense shakedown transition typical for square planar system. Figure S10 shows the  $k^3$  weighted Cu K-edge EXAFS for [Bu<sub>4</sub>N][2] along with the non-phase shift corrected Fourier transform ( $k=2\text{-}13.2 \text{ \AA}^{-1}$ ). FEFF fits are presented in Table S3, which are consistent with 3 Cu-N/O at 1.96 Å and 1 Cu-Cl at 2.21 Å. The second and third shells were fit with single and multiple scattering contributions from the nitrogenous ligand system. The bond distances for [Bu<sub>4</sub>N][2] and [Bu<sub>4</sub>N][3] are in good agreement with those obtained from x-ray diffraction and indicate that the sample integrity is retained in solution.

**Procedure for the kinetic measurements of the reaction of 4 with substrates and the product analysis:** Kinetic analysis of the reaction of 4 with DHA was monitored by UV-vis spectroscopy and performed as described above, recording a spectrum every 5 seconds for reactions run at -50 °C or colder and every 3 seconds for reactions run at -40 °C or warmer. Data were collected until there was no change in the spectrum for at least 5 minutes. The kinetic trace was determined by the disappearance of the UV-vis feature due to 4 at 540 nm and was corrected for the absorbance due to the products. The extent of the reaction,  $\lambda$ , at time  $t$  is given by the following equation:

(10) Sarangi, R.; Aboeella, N.; Fujisawa, K.; Tolman, W. B.; Hedman, B.; Hodgson, K. O.; Solomon, E. I. *J. Am. Chem. Soc.* **2006**, *128*, 8286-8296.

(11) DuBois, J. L.; Mukherjee, P.; Stack, T. D. P.; Hedman, B.; Solomon, E. I.; Hodgson, K. O. *J. Am. Chem. Soc.* **2000**, *122*, 5775-5787.

$$\lambda = \frac{A_t - A_0}{A_p - A_0} \quad (1)$$

where  $A_t$  is the absorbance at time  $t$ ,  $A_0$  is the absorbance at  $t = 0$  and  $A_p$  is the absorbance of the products at the completion of the reaction. The concentration of **4** is then determined from  $A_0^*(1-\lambda)$  and the concentration of the products is determined from  $A_p^* \lambda$ . The pseudo first order rate constant,  $k_{\text{obs}}$ , is determined from the decay of **4** as a function of time. Second order rate constants are determined based on the concentration of DHA ( $k = k_{\text{obs}}/[\text{DHA}]$ ) and are used for all Eyring plots and KIE determinations.

**Procedure for the reduction of LCuOH (4).** Stock solutions of reagents were prepared similar to those for the oxidation: 3 mM solutions of **[Bu<sub>4</sub>N][3]**, FcPF<sub>6</sub> and decamethylferrocene (Fc\*) in acetone. A 0.1 mL aliquot of the stock solution of **[Bu<sub>4</sub>N][3]** was added to a UV-vis cuvette along with 2.7 mL of acetone. After cooling the cuvette to -80 °C, 0.1 mL of the FcPF<sub>6</sub> solution was added, causing the immediate formation of an intensely purple species (**4**). This was then followed by the addition of 0.1 mL of the Fc\* solution, which immediately quenched the purple species, forming a pale green solution. Control experiments were also done omitting each of the three reagents (replacing with an additional 0.1 mL of acetone to maintain concentration). Omitting the FcPF<sub>6</sub> yielded no reaction and omitting **[Bu<sub>4</sub>N][3]** yielded a solution of Fc\*<sup>+</sup>. The UV-vis data are shown in Figure S13.

**Procedure for assaying contamination of chloride complex [PPN][2] in crystalline [PPN][3].** Three batches (A-C) of crystalline **[PPN][3]** were prepared as described above (as used to prepare samples evaluated by X-ray crystallography). Each batch was dissolved in acetone and UV-vis spectra were compared to those of pure samples of **[Bu<sub>4</sub>N][2]** and **[Bu<sub>4</sub>N][3]**. The extinction values at 400 nm (which  $\lambda_{\text{max}}$  of the former chloride complex) were measured and the data analyzed via the following equation to determine the level of chloride contamination:

$$(\varepsilon(\text{obs}) - \varepsilon(\text{OH})) / (\varepsilon(\text{Cl}) - \varepsilon(\text{OH})) = \text{extent of chloride substitution}$$

where the  $\varepsilon$ 's are the extinction values at 400 nm for the crystals ( $\varepsilon(\text{obs})$ ), **[Bu<sub>4</sub>N][3]** ( $\varepsilon(\text{OH})$ ) and **[Bu<sub>4</sub>N][2]** ( $\varepsilon(\text{Cl})$ ). Based on this data, the A sample was 26.8% chloride, the B sample was 28.4% chloride and the C sample was 22.3% chloride.

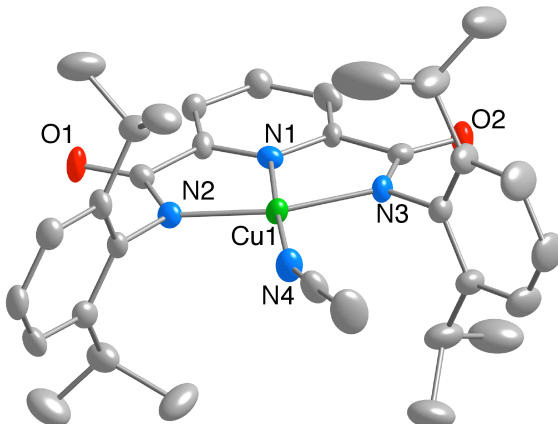


**Figure S1.** Representation of the X-ray crystal structure of LCu(CH<sub>3</sub>CN) (**1**), shown as 50% thermal ellipsoids (H atoms omitted for clarity). For details, including interatomic distances and angles, see the CIF.

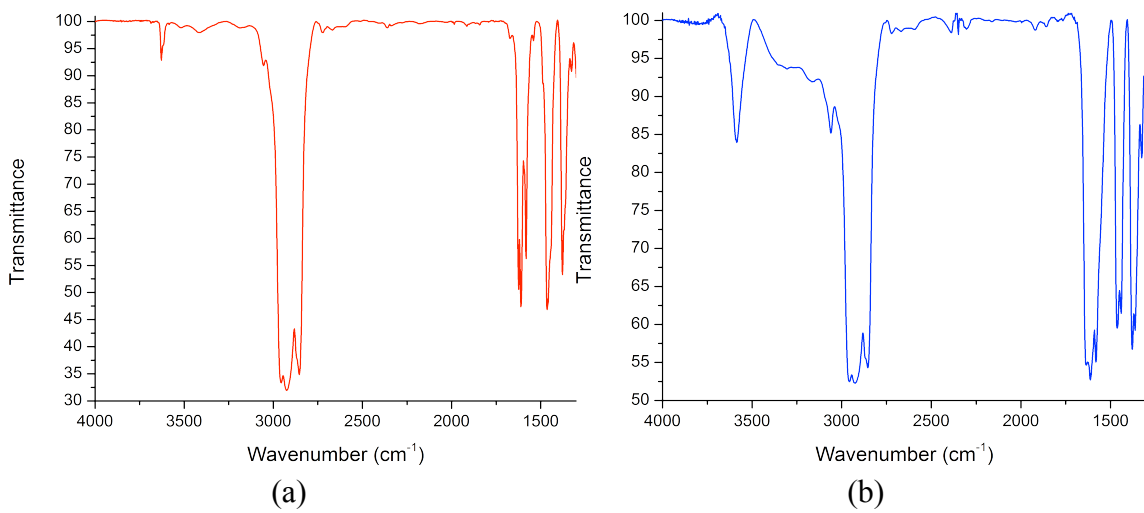


**Figure S2.** FTIR spectra (nujol) of (a)  $[\text{Bu}_4\text{N}][3]$  and (b) **5**.

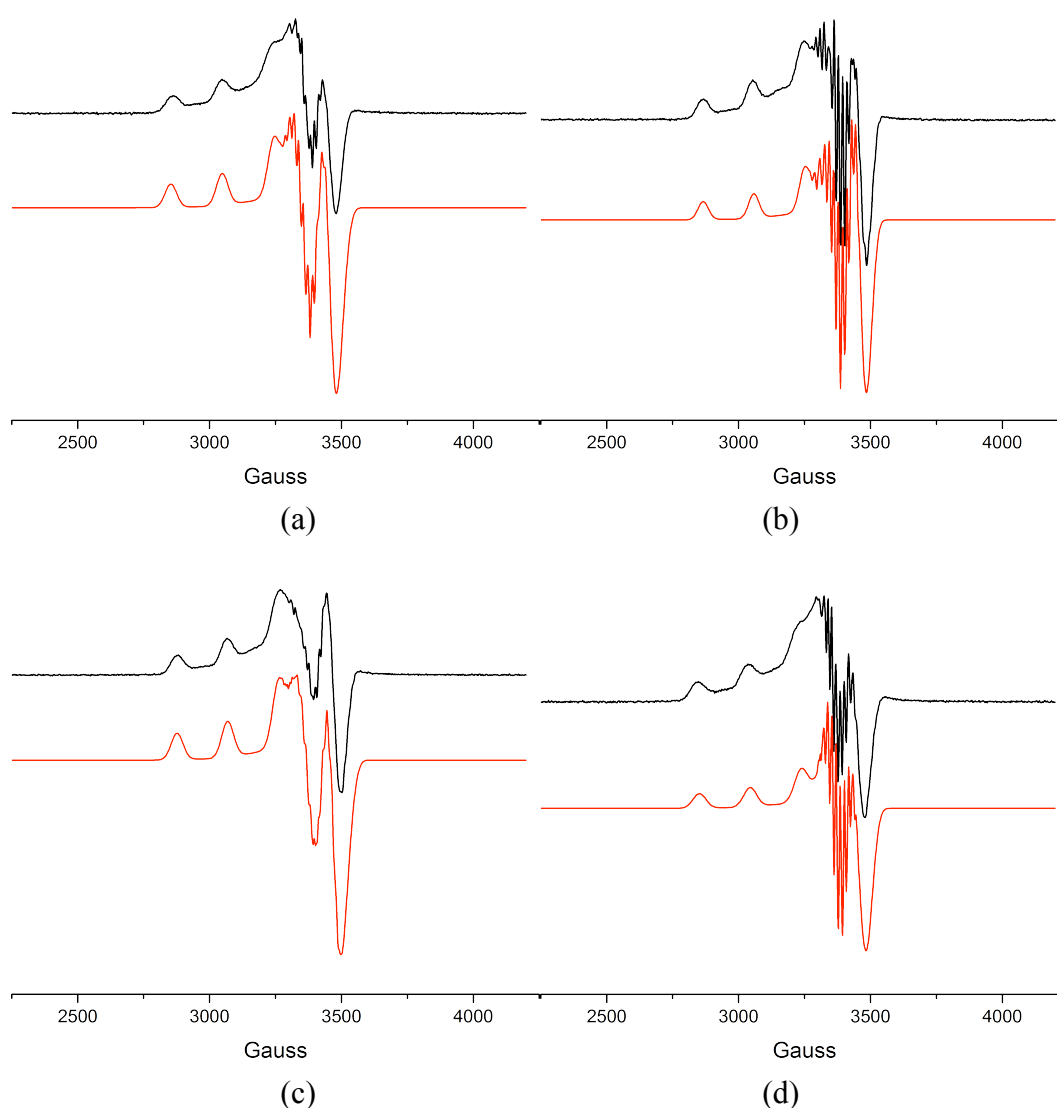


**Figure S3.** EPR spectra (black) and simulations (red) of (a) **1**, (b)  $[\text{Bu}_4\text{N}][\mathbf{3}]$ , (c)  $[\text{Bu}_4\text{N}][\mathbf{2}]$ , and (d) **5**. All spectra measured for solutions in 3:1 toluene/acetone.

**Table S1.** Summary of simulated EPR parameters ( $A$  units  $\times 10^{-4} \text{ cm}^{-1}$ ).

| Compound                            | $g(x)$ | $g(y)$ | $g(z)$ | $A(\text{Cu})$ | $A(\text{N}_{\text{amide}})$ | $A(\text{N}_{\text{py}})$ | $A(\text{Cl})$ |
|-------------------------------------|--------|--------|--------|----------------|------------------------------|---------------------------|----------------|
| <b>1</b>                            | 2.027  | 2.064  | 2.190  | 199            | 18.8                         | 14                        |                |
| $[\text{Bu}_4\text{N}][\mathbf{2}]$ | 2.016  | 2.054  | 2.177  | 195            | 18.2                         | 15.3                      | 15.3           |
| $[\text{Bu}_4\text{N}][\mathbf{3}]$ | 2.032  | 2.055  | 2.185  | 196            | 17.7                         | 13.4                      |                |
| <b>5</b>                            | 2.020  | 2.056  | 2.195  | 197            | 15.8                         | 13.0                      |                |

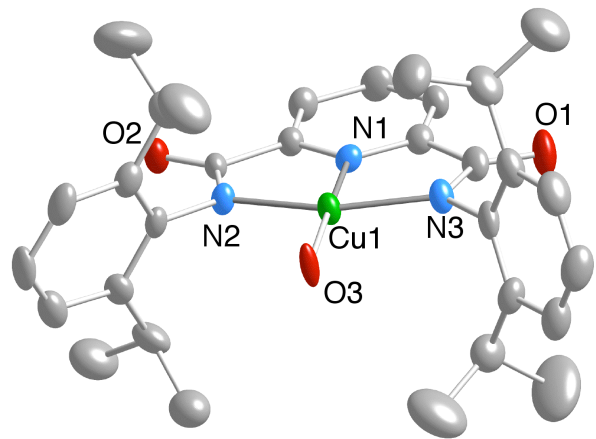


**Figure S4.** Representation of the X-ray crystal structure of the anionic portion of  $[\text{PPN}][\mathbf{3}]$ , shown as 50% thermal ellipsoids (H atoms omitted for clarity). For details, including interatomic distances and angles, see the CIF.

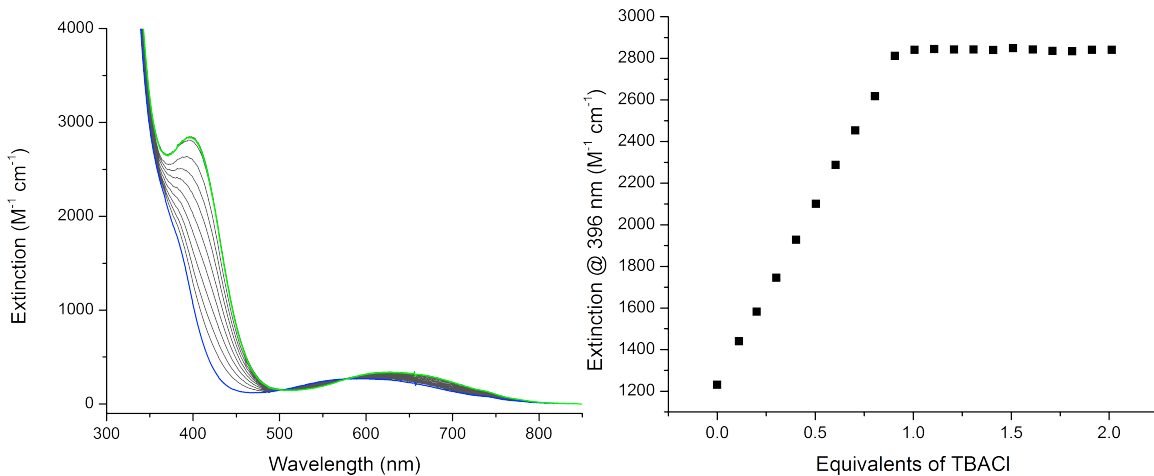


**Figure S5.** (left) UV-vis spectra showing the conversion of  $[\text{Bu}_4\text{N}][\mathbf{3}]$  (blue) to  $[\text{Bu}_4\text{N}][\mathbf{2}]$  (green) by the addition of aliquots of  $\text{Bu}_4\text{NCl}$  in acetone at  $-80^\circ\text{C}$ . (right) Titration data monitoring the conversion at 396 nm, showing the completion of reaction upon addition of 1 equiv.  $\text{Bu}_4\text{NCl}$ .

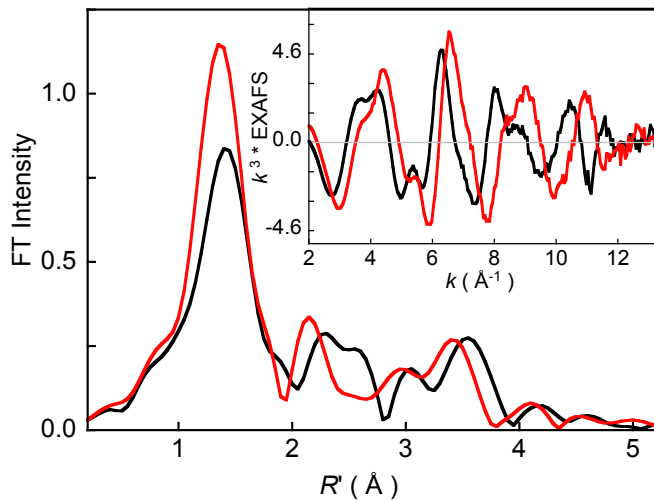


**Figure S6.** The  $k^3$  weighted Cu K-edge EXAFS (inset) and their corresponding non-phase shift corrected Fourier transforms for [Bu<sub>4</sub>N][3] (—) and 4 (—).

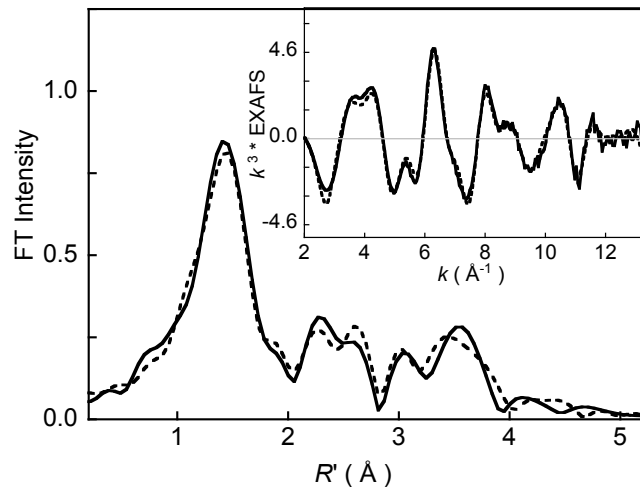


**Figure S7.** The  $k^3$  weighted Cu K-edge EXAFS (inset) and their corresponding non-phase shift corrected Fourier transforms for [Bu<sub>4</sub>N][3]. Data (—), Fit (---).

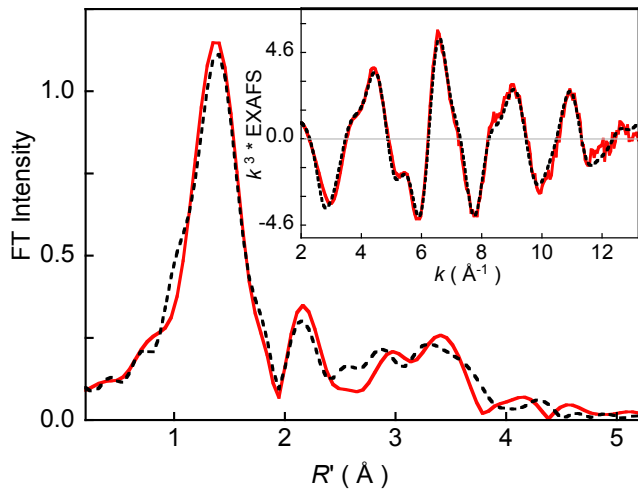


**Figure S8.** The  $k^3$  weighted Cu K-edge EXAFS (inset) and their corresponding non-phase shift corrected Fourier transforms for **4**. Data (—), Fit (---).

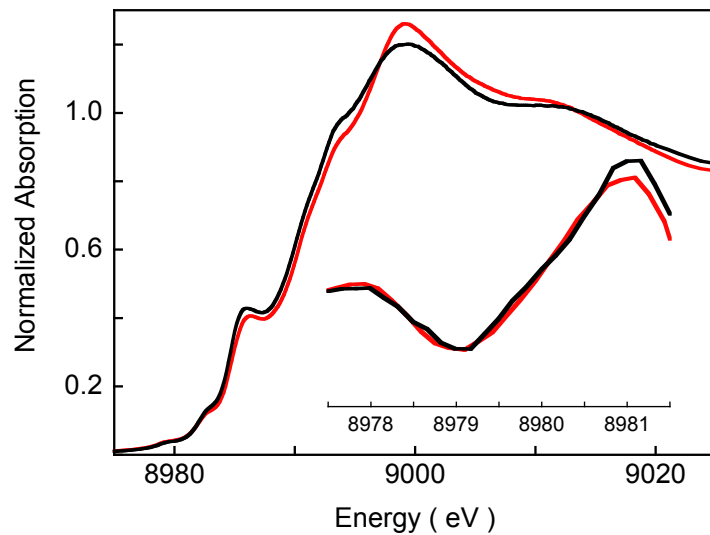


**Figure S9.** The normalized Cu K-edge XAS spectra of  $[\text{Bu}_4\text{N}] [\mathbf{3}]$  (—) and  $[\text{Bu}_4\text{N}] [\mathbf{2}]$  (—). The inset shows the second derivative spectra of the pre-edge region.

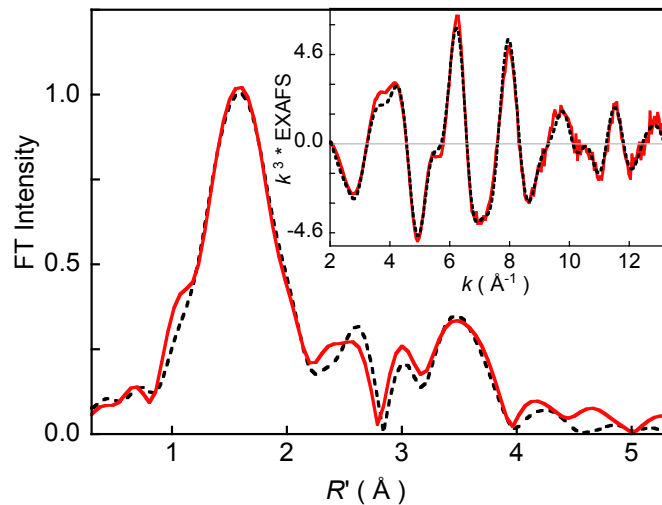


**Figure S10.** The  $k^3$  weighted Cu K-edge EXAFS (inset) and their corresponding non-phase shift corrected Fourier transforms for  $[\text{Bu}_4\text{N}][\mathbf{2}]$ . Data (—), Fit (---).

**Table S2.** Cu-K Pre-edge Analysis.

|                                     | Pre-edge<br>( $1s \rightarrow 3d$ ) (eV) <sup>a</sup> | Cu K-edge<br>Maxima (eV) |
|-------------------------------------|---|--------------------------|
| $[\text{Bu}_4\text{N}][\mathbf{2}]$ | 8979.1  | 8999.1                   |
| $[\text{Bu}_4\text{N}][\mathbf{3}]$ | 8979.1  | 8999.3                   |
| <b>4</b>                            | 8980.8  | 9000.4                   |

<sup>a</sup>Accuracy of measurement is <0.05 eV on SSRL beamline 7-3. Pre-edge positions estimated from second derivatives obtained in Kaleidagraph.

**Table S3.** EXAFS Least Squares Fitting Results

| Complex                             | Coordination/Path | R(Å) <sup>a</sup> | $\sigma^2(\text{\AA}^2)$ <sup>b</sup> | $E_0$ (eV) | $F^c$ |
|-------------------------------------|-------------------|-------------------|---------------------------------------|------------|-------|
| $[\text{Bu}_4\text{N}][\mathbf{2}]$ | 3 Cu-N/O          | 1.98              | 423                                   | -6.94      | 0.13  |
|                                     | 1 Cu-Cl           | 2.21              | 272                                   |            |       |
|                                     | 4 Cu-C            | 2.85              | 315                                   |            |       |
|                                     | 2 Cu-C            | 3.06              | 207                                   |            |       |
|                                     | 12 Cu-C-N         | 3.07              | 395                                   |            |       |
|                                     | 16 Cu-C-N         | 4.17              | 275                                   |            |       |
|                                     | 12 Cu-C-N         | 4.76              | 949                                   |            |       |
| $[\text{Bu}_4\text{N}][\mathbf{3}]$ | 4 Cu-N/O          | 1.95              | 737                                   | -6.47      | 0.12  |
|                                     | 4 Cu-C            | 2.85              | 359                                   |            |       |
|                                     | 2 Cu-C            | 3.07              | 586                                   |            |       |
|                                     | 12 Cu-C-N         | 3.10              | 912                                   |            |       |
|                                     | 16 Cu-C-N         | 4.18              | 467                                   |            |       |
|                                     | 12 Cu-C-N         | 4.67              | 1139                                  |            |       |

|   |           |      |      |       |      |
|---|-----------|------|------|-------|------|
| 4 | 4 Cu-N/O  | 1.86 | 537  | -7.71 | 0.16 |
|   | 4 Cu-C    | 2.75 | 323  |       |      |
|   | 2 Cu-C    | 2.94 | 317  |       |      |
|   | 12 Cu-C-N | 3.01 | 222  |       |      |
|   | 16 Cu-C-N | 4.05 | 565  |       |      |
|   | 12 Cu-C-N | 4.54 | 1180 |       |      |

<sup>a</sup>The estimated standard deviations for the distances are in the order of  $\pm 0.02 \text{ \AA}$ . <sup>b</sup>The  $\sigma^2$  values are multiplied by  $10^5$ . <sup>c</sup>Error is given by  $\Sigma[(\chi_{\text{obsd}} - \chi_{\text{calcd}})^2 k^6]/\Sigma[(\chi_{\text{obsd}})^2 k^6]$ . <sup>d</sup>The  $\sigma^2$  factor of the multiple scattering path is linked to that of the corresponding single scattering path.

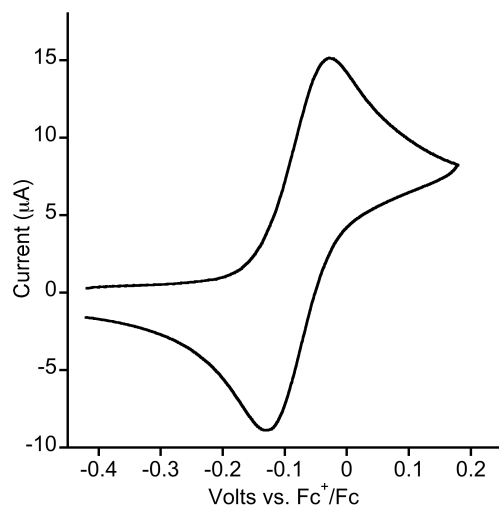


**Figure S11.** Cyclic voltammogram of  $[\text{Bu}_4\text{N}][\mathbf{3}]$  in acetone (0.1 M  $\text{Bu}_4\text{NPF}_6$ ).

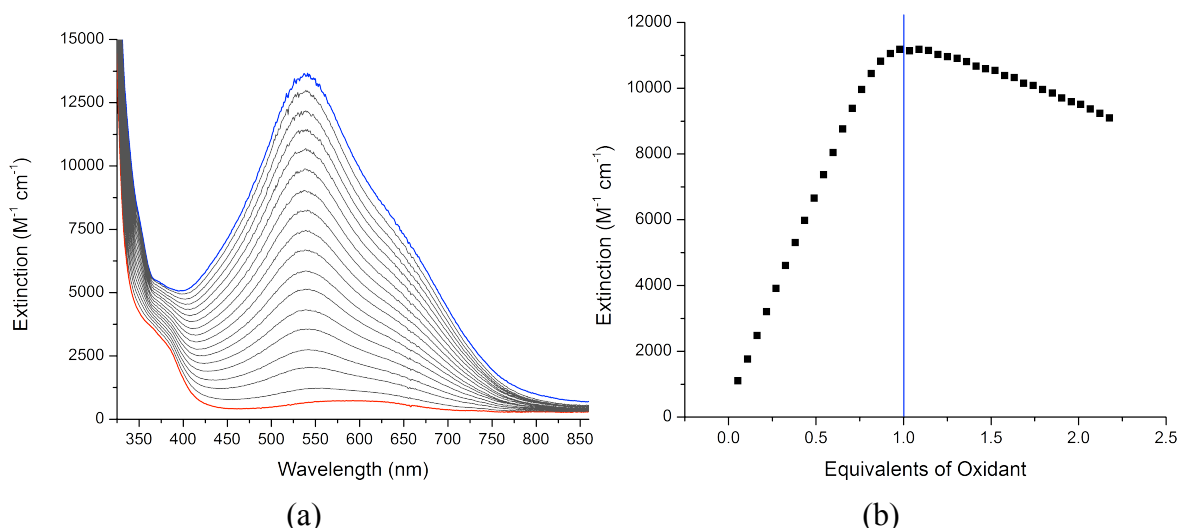


**Figure S12.** Titration data for reaction of  $[\text{Bu}_4\text{N}][\mathbf{3}]$  with  $\text{Fc}^+\text{PF}_6^-$  at  $-80^\circ\text{C}$ . (a) UV-vis spectroscopic changes as equivalents of  $\text{Fc}^+\text{PF}_6^-$  are added to  $[\text{Bu}_4\text{N}][\mathbf{3}]$  (red = starting spectrum, blue = ending spectrum). (b) Extinction at 540 nm as a function of equiv oxidant added to  $[\text{Bu}_4\text{N}][\mathbf{3}]$ .

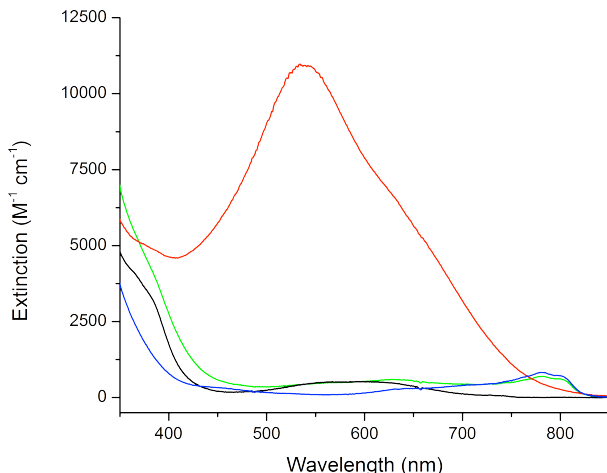


**Figure S13.** UV-vis spectra in acetone at  $-80\text{ }^{\circ}\text{C}$  of  $[\text{Bu}_4\text{N}]$ **[3]** (black), the product of reaction with  $\text{FcPF}_6$ , **4** (red), after subsequent reduction with  $\text{Fc}^*$  (green), and the control spectrum of  $\text{FcPF}_6 + \text{Fc}^*$  (blue).

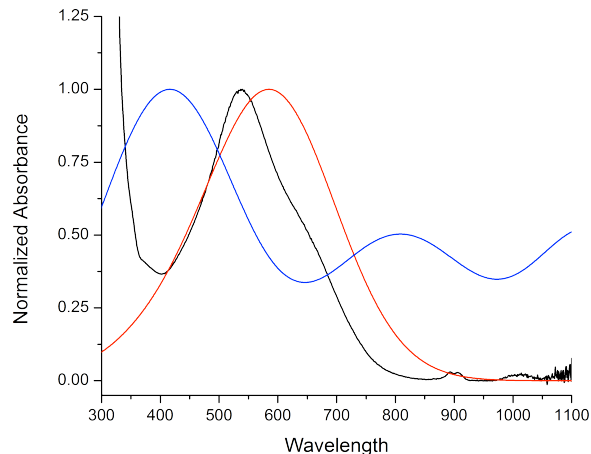


**Figure S14.** Calculated UV-vis spectra from TD-DFT calculations for **4**. Spectra shown are experimental (black), singlet state (red) and triplet state (blue).

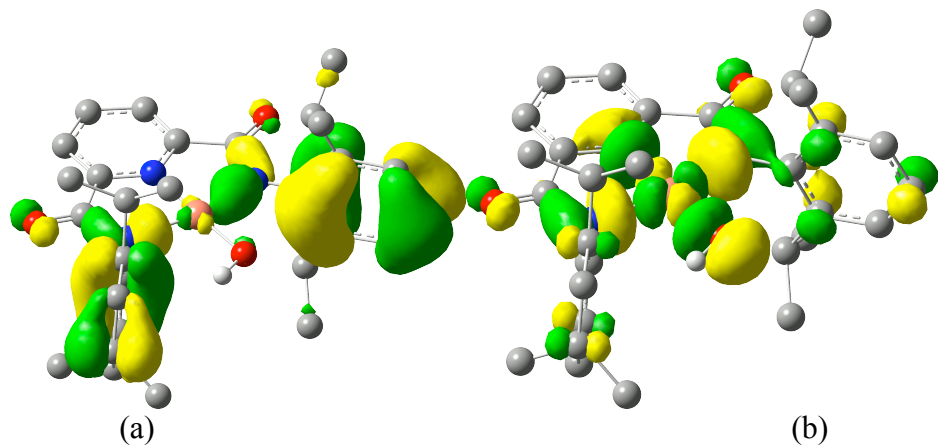


**Figure S15.** TD-DFT orbitals involved in the calculated transition at 589 nm. The transition is from (a) to (b).

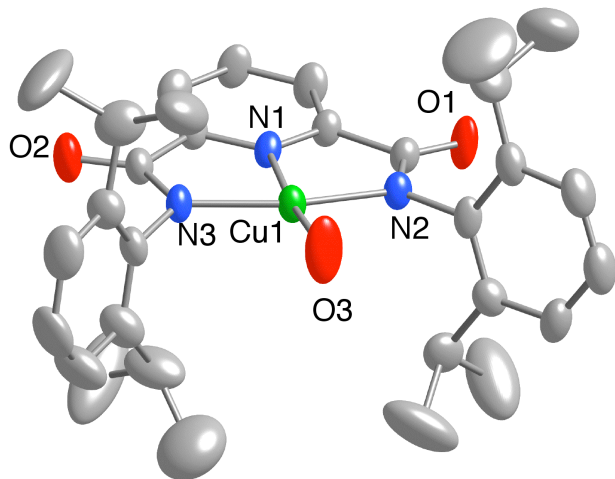


**Figure S16.** Representation of the X-ray crystal structure of **5**, shown as 50% thermal ellipsoids (H atoms omitted for clarity). For details, including interatomic distances and angles, see the CIF.

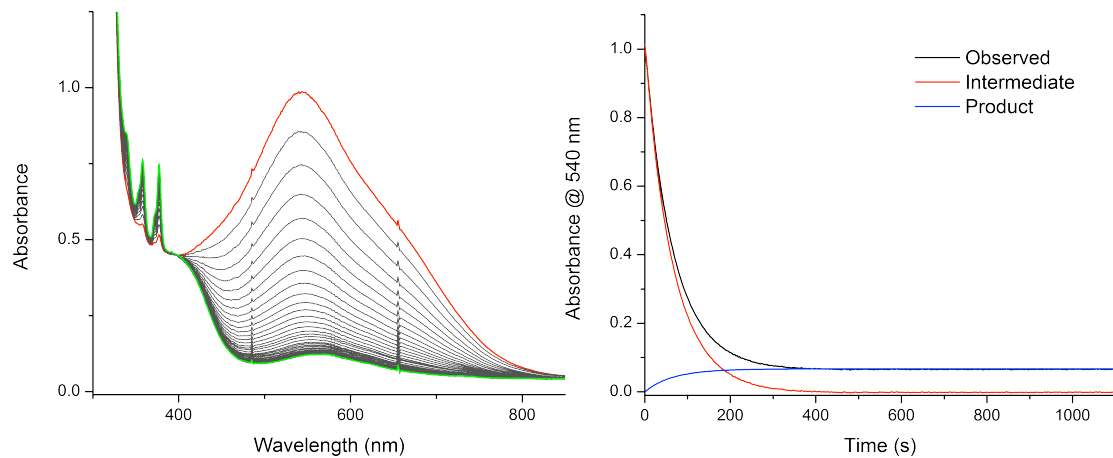


**Figure S17.** (left) Change in the UV-vis spectrum of **4** (red to green) in the presence of 10 equivalents of DHA in acetone at -40 °C. (right) Representative deconvolution of the observed absorbance at 540 nm (black) into components **4** (red) and **5** (blue). Rate constants were determined by modeling the rate of decay of the red curve.

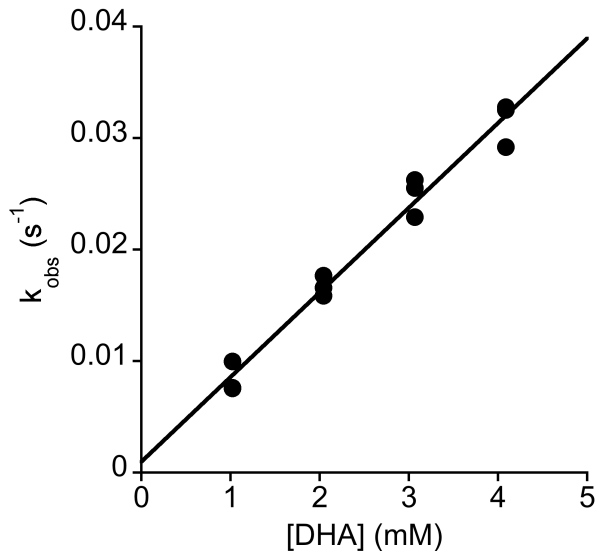


**Figure S18.** Linear relationship between pseudo first order constant ( $k_{\text{obs}}$ , three replicates) and the initial concentration of DHA (10-40 equivalents used, based on 0.1 mM Cu in the reaction). Reactions were performed at -60 °C in acetone. Regression equation:  $k_{\text{obs}} = 7.66 \times 10^{-3} [\text{DHA}] + 9.07 \times 10^{-4}$  ( $r^2 = 0.996$ ). The initial rate of the decay of **4** was measured at -80 °C and found to proceed with a rate constant of  $1.35 \times 10^{-4} \text{ M}^{-1} \text{ s}^{-1}$  which agrees with the intercept of the regression function.

**Table S4.** Rate constants used to construct the Eyring plot (Figure 4 in text).

| Temp. (°C)  | k <sub>H</sub> Run 1 | k <sub>H</sub> Run 2 | k <sub>H</sub> Run 3 | Average | Std Dev        |
|---|----------------------|----------------------|----------------------|---------|----------------|
| -30   | 24.56282             | 24.41563             | 23.50446             | 24.2    | 0.57           |
| -40   | 14.82068             | 14.01603             | 13.12566             | 14.0    | 0.85           |
| -50   | 7.02495              | 9.24107              | 8.68149              | 8.3     | 1.15           |
| -60   | 4.02513              | 4.17551              | 5.28693              | 4.5     | 0.69           |
| -70   | 2.3145               | 1.95966              | 2.18854              | 2.2     | 0.17           |
| -80   | 1.04511              | 1.01551              | 1.12631              | 1.06    | 0.057          |
| Regression equation: $\ln(k/T) = -2713.3 (1/T) + 8.839$ |                      |                      |                      |         | $r^2 = 0.9998$ |
| k <sub>D</sub> Run 1                                    | k <sub>D</sub> Run 2 | k <sub>D</sub> Run 3 | Average              | Std Dev |                |
| 0.69193   | 0.58284              | 0.62588              | 0.63                 | 0.055   |                |
| 0.3187  | 0.33527              | 0.33405              | 0.329                | 0.0092  |                |
| 0.18412   | 0.21211              | 0.17629              | 0.19                 | 0.019   |                |
| 0.07303   | 0.06489              | 0.07075              | 0.069                | 0.0042  |                |
| 0.04916   | 0.05111              | -----                | 0.050                | 0.0014  |                |
| Regression equation: $\ln(k/T) = -2827.5 (1/T) + 5.559$ |                      |                      |                      |         | $r^2 = 0.981$  |

<sup>a</sup> For k<sub>H</sub> runs, 10 equiv DHA used. For k<sub>D</sub> runs, 200 equiv DHA-d<sub>4</sub> used. All units for k values are M<sup>-1</sup>s<sup>-1</sup>.

## Computational Details

DFT geometry optimizations were performed on complexes of the full, untruncated ligand using the mPW functional<sup>12</sup> implemented in Gaussian09.<sup>13</sup> A mixed basis set comprised of 6-311+g(d,p) on C, H, N and O and the Stuttgart/Dresden basis set and pseudopotential (SDD) on Cu (including 2 f-functions with coefficients 5.208 and 1.315). Final optimizations were performed with no frozen coordinates. Solvation effects were included by performing single point energies on optimized structures using the SMD solvation model in acetone. Energy minima and transition states were identified through frequency analysis. Time dependant DFT (TDDFT) calculations were performed using the B98 functional<sup>14</sup> in Gaussian09 with the 6-31+G(d,p) basis sets on C, H, N and O and the SDD basis set/pseudopotential as previously described on Cu.

The structure of **3**<sup>-</sup> and singlet state of **4** were located in the Cs space group with the hydroxide hydrogen coplanar with the ligand as the lowest energy structure. The triplet state of **4** distorted from a square planar structure with the hydroxide ~10 degrees out of the square plane; however it could only be located as a rotational transition state with the hydroxide hydrogen perpendicular to the ligand plane. This transition state was also located for **3**<sup>-</sup> and the singlet state of **4** where it was found that the rotational barrier was fairly small on the scale of the calculated singlet/triplet energy gap.

**Table S5.** Summary of Energetic Results

| Structure   | Relative Gas Phase G | Relative Solvated G |
|---|----------------------|---------------------|
| <b>3</b> <sup>-</sup> [LCuOH] <sup>-</sup> doublet    | ---                  | ---                 |
| <b>3</b> <sup>-</sup> [LCuOH] <sup>-</sup> doublet TS | 2.7 kcal/mol         | 3.5 kcal/mol        |
| <b>4</b> LCuOH singlet                                | ---                  | ---                 |
| <b>4</b> LCuOH singlet TS                             | 2.5 kcal/mol         | 2.0 kcal/mol        |
| <b>4</b> LCuOH triplet TS                             | 19.9 kcal/mol        | 21.0 kcal/mol       |

## TDDFT Transitions

UV-vis transition energies were calculated for the first 36 states for both the singlet and triplet wavefunctions as described above. Key transitions are bolded and described below.

(12) (a) Perdew, J. P. Unified Theory of Exchange and Correlation Beyond the Local Density Approximation. In *Electronic Structure of Solids '91*; Ziesche, P., Eschrig, H., Eds.; Akademie Verlag: Berlin, 1991, pp 11-20; (b) Perdew, J.; Wang, Y. *Phys. Rev. B* **1992**, *45*, 13244-13249. (c) Adamo, C.; Barone, V. *J. Chem. Phys.* **1998**, *108*, 664-675.

(13) M. J. Frisch, G. W. Trucks, H. B. Schlegel, G. E. Scuseria, M. A. Robb, J. R. Cheeseman, G. Scalmani, V. Barone, B. Mennucci, G. A. Petersson, H. Nakatsuji, M. Caricato, X. Li, H. P. Hratchian, A. F. Izmaylov, J. Bloino, G. Zheng, J. L. Sonnenberg, M. Hada, M. Ehara, K. Toyota, R. Fukuda, J. Hasegawa, M. Ishida, T. Nakajima, Y. Honda, O. Kitao, H. Nakai, T. Vreven, J. A. Montgomery, Jr., J. E. Peralta, F. Ogliaro, M. Bearpark, J. J. Heyd, E. Brothers, K. N. Kudin, V. N. Staroverov, R. Kobayashi, J. Normand, K. Raghavachari, A. Rendell, J. C. Burant, S. S. Iyengar, J. Tomasi, M. Cossi, N. Rega, J. M. Millam, M. Klene, J. E. Knox, J. B. Cross, V. Bakken, C. Adamo, J. Jaramillo, R. Gomperts, R. E. Stratmann, O. Yazyev, A. J. Austin, R. Cammi, C. Pomelli, J. W. Ochterski, R. L. Martin, K. Morokuma, V. G. Zakrzewski, G. A. Voth, P. Salvador, J. J. Dannenberg, S. Dapprich, A. D. Daniels, O. Farkas, J. B. Foresman, J. V. Ortiz, J. Cioslowski, D. J. Fox, *Gaussian 09*, Revision A.02; Gaussian, Inc.: Wallingford CT, 2009.

(14) (a) Becke, A. D. *J. Chem. Phys.* **1997**, *107*, 8554-8560. (b) Schmid, H. L.; Becke, A. D. *J. Chem. Phys.* **1998**, *108*, 9624-9631. (c) Cramer, C. J.; Truhlar, D. G. *Phys. Chem. Chem. Phys.* **2009**, *11*, 10757-10816.

Transitions were then fit to standard Gaussian curves to determine the calculated spectra shown above.

**Table S6.** LCuOH singlet

| Energy (nm)   | Oscillator Strength | Description | Energy (nm) | Oscillator Strength | Description |
|---------------|---------------------|-------------|-------------|---------------------|-------------|
| 1053.63       | 0                   |             | 441.93      | 0                   |             |
| 1007.75       | 0                   |             | 435.53      | 0.0014              |             |
| 894.65        | 0                   |             | 426.14      | 0.0231              |             |
| 821.04        | 0                   |             | 422.51      | 0                   |             |
| 707.43        | 0.0212              |             | 418.82      | 0                   |             |
| 674.29        | 0.0208              |             | 399.90      | 0                   |             |
| 640.91        | 0                   |             | 382.93      | 0                   |             |
| 630.80        | 0                   |             | 382.03      | 0.0002              |             |
| 625.11        | 0                   |             | 381.60      | 0                   |             |
| 600.40        | 0.0076              |             | 381.51      | 0                   |             |
| 598.78        | 0.0016              |             | 378.26      | 0                   |             |
| <b>589.55</b> | <b>0.2892</b>       | <b>LMCT</b> | 377.85      | 0.0008              |             |
| 559.34        | 0.002               |             | 374.80      | 0                   |             |
| 544.61        | 0                   |             | 373.22      | 0.0055              |             |
| 480.02        | 0.0414              |             | 366.08      | 0                   |             |
| 474.57        | 0                   |             | 364.88      | 0.0056              |             |
| 457.14        | 0                   |             | 362.69      | 0.0002              |             |
| 442.65        | 0                   |             | 356.65      | 0.0019              |             |

**Table S7.** LCuOH triplet

| Energy (nm)    | Oscillator Strength | Description | Energy (nm) | Oscillator Strength | Description |
|----------------|---------------------|-------------|-------------|---------------------|-------------|
| 2729.45        | 0.0004              |             | 443.86      | 0.0007              |             |
| <b>2323.03</b> | <b>0.0884</b>       |             | 443.73      | 0.0017              |             |
| 1382.7         | 0.004               |             | 416.12      | 0.0008              |             |
| 1345.44        | 0.0002              |             | 412.93      | 0.0004              |             |
| 1286.5         | 0.006               |             | 412.5       | 0.0031              |             |
| <b>1126.52</b> | <b>0.0349</b>       |             | 405.92      | 0                   |             |
| 870.7          | 0.0202              |             | 401.02      | 0.0066              |             |
| 781.68         | 0.0051              |             | 389.12      | 0.0043              |             |
| <b>742.5</b>   | <b>0.017</b>        |             | 383.45      | 0.001               |             |
| 678.8          | 0.0004              |             | 372.71      | 0.0032              |             |
| 529.09         | 0.0015              |             | 372.23      | 0.0024              |             |
| 511.29         | 0.0001              |             | 371.21      | 0.005               |             |
| 491.11         | 0.0031              |             | 370.44      | 0.001               |             |
| 484.38         | 0.0007              |             | 362.33      | 0.0018              |             |
| <b>479.68</b>  | <b>0.0142</b>       |             | 360.67      | 0.0021              |             |
| 467.34         | 0.0023              |             | 356.79      | 0.0055              |             |

|        |        |  |        |        |  |
|--------|--------|--|--------|--------|--|
| 461.97 | 0.0008 |  | 352.25 | 0.0084 |  |
| 452.58 | 0.01   |  | 345.56 | 0      |  |

### Optimized geometries

LCuOH doublet, rotational transition state

|    |           |           |           |
|----|-----------|-----------|-----------|
| Cu | 0.111431  | 0.172982  | 0.000000  |
| O  | 1.533792  | -1.053514 | 0.000000  |
| N  | -1.123514 | 1.692277  | 0.000000  |
| O  | -1.362994 | 1.829806  | 3.535274  |
| C  | -1.527091 | 2.191782  | 1.176774  |
| C  | -2.382319 | 3.297777  | 1.215241  |
| H  | -2.694214 | 3.682972  | 2.185498  |
| C  | -2.803466 | 3.853979  | 0.000000  |
| H  | -3.469777 | 4.719297  | 0.000000  |
| C  | -2.382319 | 3.297777  | -1.215241 |
| H  | -2.694214 | 3.682972  | -2.185498 |
| C  | -1.527091 | 2.191782  | -1.176774 |
| C  | -1.017895 | 1.447759  | 2.396799  |
| N  | -0.229777 | 0.404577  | 2.047100  |
| C  | 0.288046  | -0.440364 | 3.061533  |
| C  | -0.502678 | -1.506542 | 3.570117  |
| C  | 0.047294  | -2.355859 | 4.541104  |
| H  | -0.557147 | -3.173212 | 4.942066  |
| C  | 1.352256  | -2.177428 | 5.006009  |
| H  | 1.764858  | -2.850013 | 5.761368  |
| C  | 2.125158  | -1.133760 | 4.493073  |
| H  | 3.148480  | -0.997521 | 4.851397  |
| C  | 1.616988  | -0.256196 | 3.524727  |
| C  | -1.935641 | -1.723032 | 3.094556  |
| H  | -2.085504 | -1.064092 | 2.226904  |
| C  | -2.949639 | -1.302115 | 4.179305  |
| H  | -2.777089 | -0.260613 | 4.481882  |
| H  | -2.857828 | -1.941949 | 5.071981  |
| H  | -3.982083 | -1.392639 | 3.803758  |
| C  | -2.189984 | -3.168230 | 2.624060  |
| H  | -1.476159 | -3.463678 | 1.841762  |
| H  | -3.207330 | -3.264797 | 2.212917  |
| H  | -2.099023 | -3.889198 | 3.451565  |
| C  | 2.491083  | 0.871891  | 2.990734  |
| H  | 1.888097  | 1.415575  | 2.249810  |
| C  | 2.873592  | 1.869222  | 4.103219  |
| H  | 1.977934  | 2.275228  | 4.594770  |
| H  | 3.450343  | 2.709738  | 3.684632  |
| H  | 3.496711  | 1.390345  | 4.875592  |
| C  | 3.731240  | 0.323148  | 2.258864  |
| H  | 4.323309  | 1.149231  | 1.832329  |
| H  | 3.415015  | -0.342615 | 1.443415  |

|   |           |           |           |
|---|-----------|-----------|-----------|
| H | 4.386766  | -0.237571 | 2.945084  |
| N | -0.229777 | 0.404577  | -2.047100 |
| O | -1.362994 | 1.829806  | -3.535274 |
| C | -1.017895 | 1.447759  | -2.396799 |
| C | 0.288046  | -0.440364 | -3.061533 |
| C | -0.502678 | -1.506542 | -3.570117 |
| C | 0.047294  | -2.355859 | -4.541104 |
| H | -0.557147 | -3.173212 | -4.942066 |
| C | 1.352256  | -2.177428 | -5.006009 |
| H | 1.764858  | -2.850013 | -5.761368 |
| C | 2.125158  | -1.133760 | -4.493073 |
| H | 3.148480  | -0.997521 | -4.851397 |
| C | 1.616988  | -0.256196 | -3.524727 |
| C | -1.935641 | -1.723032 | -3.094556 |
| H | -2.085504 | -1.064092 | -2.226904 |
| C | -2.189984 | -3.168230 | -2.624060 |
| H | -1.476159 | -3.463678 | -1.841762 |
| H | -2.099023 | -3.889198 | -3.451565 |
| H | -3.207330 | -3.264797 | -2.212917 |
| C | -2.949639 | -1.302115 | -4.179305 |
| H | -2.777089 | -0.260613 | -4.481882 |
| H | -3.982083 | -1.392639 | -3.803758 |
| H | -2.857828 | -1.941949 | -5.071981 |
| C | 2.491083  | 0.871891  | -2.990734 |
| H | 1.888097  | 1.415575  | -2.249810 |
| C | 3.731240  | 0.323148  | -2.258864 |
| H | 3.415015  | -0.342615 | -1.443415 |
| H | 4.323309  | 1.149231  | -1.832329 |
| H | 4.386766  | -0.237571 | -2.945084 |
| C | 2.873592  | 1.869222  | -4.103219 |
| H | 1.977934  | 2.275228  | -4.594770 |
| H | 3.496711  | 1.390345  | -4.875592 |
| H | 3.450343  | 2.709738  | -3.684632 |
| H | 1.202931  | -1.965516 | 0.000000  |

#### LCuOH doublet, rotational minimum

|    |           |           |          |
|----|-----------|-----------|----------|
| Cu | 0.097033  | 0.036832  | 0.000000 |
| O  | -1.764073 | 0.129288  | 0.000000 |
| N  | 2.043270  | 0.002746  | 0.000000 |
| O  | 2.228999  | -3.540845 | 0.000000 |
| C  | 2.666088  | -1.185730 | 0.000000 |
| C  | 4.062754  | -1.247236 | 0.000000 |
| H  | 4.543660  | -2.224898 | 0.000000 |
| C  | 4.780636  | -0.043198 | 0.000000 |
| H  | 5.872546  | -0.061517 | 0.000000 |
| C  | 4.103054  | 1.183499  | 0.000000 |
| H  | 4.614826  | 2.145426  | 0.000000 |

|   |           |           |           |
|---|-----------|-----------|-----------|
| C | 2.704653  | 1.169669  | 0.000000  |
| C | 1.743493  | -2.389034 | 0.000000  |
| N | 0.442362  | -2.014489 | 0.000000  |
| C | -0.572589 | -3.004030 | 0.000000  |
| C | -1.105379 | -3.472025 | 1.232530  |
| C | -2.140979 | -4.417453 | 1.206632  |
| H | -2.551954 | -4.787591 | 2.148455  |
| C | -2.658197 | -4.894285 | 0.000000  |
| H | -3.465303 | -5.630090 | 0.000000  |
| C | -2.140979 | -4.417453 | -1.206632 |
| H | -2.551954 | -4.787591 | -2.148455 |
| C | -1.105379 | -3.472025 | -1.232530 |
| C | -0.532637 | -2.987888 | 2.559821  |
| H | 0.045473  | -2.078603 | 2.337853  |
| C | 0.445112  | -4.031377 | 3.143232  |
| H | 1.230884  | -4.278465 | 2.416526  |
| H | -0.086657 | -4.961448 | 3.402296  |
| H | 0.921731  | -3.647219 | 4.059755  |
| C | -1.618146 | -2.606302 | 3.582427  |
| H | -2.307814 | -1.857678 | 3.168128  |
| H | -1.154783 | -2.178904 | 4.485276  |
| H | -2.209907 | -3.479095 | 3.900764  |
| C | -0.532637 | -2.987888 | -2.559821 |
| H | 0.045473  | -2.078603 | -2.337853 |
| C | 0.445112  | -4.031377 | -3.143232 |
| H | 1.230884  | -4.278465 | -2.416526 |
| H | 0.921731  | -3.647219 | -4.059755 |
| H | -0.086657 | -4.961448 | -3.402296 |
| C | -1.618146 | -2.606302 | -3.582427 |
| H | -1.154783 | -2.178904 | -4.485276 |
| H | -2.307814 | -1.857678 | -3.168128 |
| H | -2.209907 | -3.479095 | -3.900764 |
| N | 0.510169  | 2.073018  | 0.000000  |
| O | 2.352507  | 3.535838  | 0.000000  |
| C | 1.823061  | 2.404841  | 0.000000  |
| C | -0.463082 | 3.104173  | 0.000000  |
| C | -0.972413 | 3.595932  | 1.230127  |
| C | -1.963242 | 4.587508  | 1.205880  |
| H | -2.361808 | 4.969090  | 2.149134  |
| C | -2.456135 | 5.091045  | 0.000000  |
| H | -3.227928 | 5.864124  | 0.000000  |
| C | -1.963242 | 4.587508  | -1.205880 |
| H | -2.361808 | 4.969090  | -2.149134 |
| C | -0.972413 | 3.595932  | -1.230127 |
| C | -0.499860 | 3.020892  | 2.560010  |
| H | 0.358831  | 2.371344  | 2.339219  |
| C | -1.599597 | 2.133541  | 3.180376  |

|   |           |           |           |
|---|-----------|-----------|-----------|
| H | -1.909168 | 1.355941  | 2.467275  |
| H | -2.487017 | 2.732522  | 3.441741  |
| H | -1.236154 | 1.648035  | 4.100999  |
| C | -0.019595 | 4.106656  | 3.541096  |
| H | 0.776357  | 4.717738  | 3.092153  |
| H | 0.376075  | 3.645110  | 4.460076  |
| H | -0.839272 | 4.780061  | 3.838142  |
| C | -0.499860 | 3.020892  | -2.560010 |
| H | 0.358831  | 2.371344  | -2.339219 |
| C | -1.599597 | 2.133541  | -3.180376 |
| H | -1.909168 | 1.355941  | -2.467275 |
| H | -1.236154 | 1.648035  | -4.100999 |
| H | -2.487017 | 2.732522  | -3.441741 |
| C | -0.019595 | 4.106656  | -3.541096 |
| H | 0.776357  | 4.717738  | -3.092153 |
| H | -0.839272 | 4.780061  | -3.838142 |
| H | 0.376075  | 3.645110  | -4.460076 |
| H | -2.113050 | -0.778119 | 0.000000  |

LCuOH restricted singlet, rotational transition state

|    |           |           |           |
|----|-----------|-----------|-----------|
| Cu | -0.047838 | 0.248997  | 0.000000  |
| O  | 1.163534  | -1.114640 | 0.000000  |
| N  | -1.112884 | 1.796727  | 0.000000  |
| O  | -1.204302 | 1.859194  | 3.521809  |
| C  | -1.462296 | 2.316182  | 1.180830  |
| C  | -2.232364 | 3.479641  | 1.218556  |
| H  | -2.512609 | 3.896263  | 2.185428  |
| C  | -2.613633 | 4.060034  | 0.000000  |
| H  | -3.215001 | 4.970050  | 0.000000  |
| C  | -2.232364 | 3.479641  | -1.218556 |
| H  | -2.512609 | 3.896263  | -2.185428 |
| C  | -1.462296 | 2.316182  | -1.180830 |
| C  | -0.958255 | 1.518786  | 2.361391  |
| N  | -0.241230 | 0.424939  | 1.947585  |
| C  | 0.299288  | -0.490034 | 2.882998  |
| C  | -0.503211 | -1.570293 | 3.346557  |
| C  | 0.051901  | -2.454528 | 4.279333  |
| H  | -0.549741 | -3.281754 | 4.659684  |
| C  | 1.362729  | -2.294921 | 4.736072  |
| H  | 1.776043  | -2.996741 | 5.462519  |
| C  | 2.144481  | -1.240547 | 4.260602  |
| H  | 3.168275  | -1.127805 | 4.621162  |
| C  | 1.639554  | -0.326171 | 3.327779  |
| C  | -1.945631 | -1.752361 | 2.888974  |
| H  | -2.108104 | -1.071284 | 2.040127  |
| C  | -2.931392 | -1.345196 | 4.006085  |
| H  | -2.743761 | -0.317336 | 4.343624  |

|   |           |           |           |
|---|-----------|-----------|-----------|
| H | -2.833233 | -2.012318 | 4.876087  |
| H | -3.969864 | -1.411274 | 3.646647  |
| C | -2.231505 | -3.183542 | 2.393986  |
| H | -1.532669 | -3.484951 | 1.600565  |
| H | -3.253607 | -3.250088 | 1.992247  |
| H | -2.150785 | -3.919954 | 3.207108  |
| C | 2.512812  | 0.820085  | 2.837902  |
| H | 1.956686  | 1.337168  | 2.042727  |
| C | 2.770421  | 1.841483  | 3.966526  |
| H | 1.827452  | 2.221324  | 4.383170  |
| H | 3.350629  | 2.695600  | 3.585083  |
| H | 3.344751  | 1.387386  | 4.788373  |
| C | 3.831224  | 0.313471  | 2.221712  |
| H | 4.405295  | 1.155720  | 1.806769  |
| H | 3.630509  | -0.403039 | 1.414467  |
| H | 4.466946  | -0.179513 | 2.972629  |
| N | -0.241230 | 0.424939  | -1.947585 |
| O | -1.204302 | 1.859194  | -3.521809 |
| C | -0.958255 | 1.518786  | -2.361391 |
| C | 0.299288  | -0.490034 | -2.882998 |
| C | -0.503211 | -1.570293 | -3.346557 |
| C | 0.051901  | -2.454528 | -4.279333 |
| H | -0.549741 | -3.281754 | -4.659684 |
| C | 1.362729  | -2.294921 | -4.736072 |
| H | 1.776043  | -2.996741 | -5.462519 |
| C | 2.144481  | -1.240547 | -4.260602 |
| H | 3.168275  | -1.127805 | -4.621162 |
| C | 1.639554  | -0.326171 | -3.327779 |
| C | -1.945631 | -1.752361 | -2.888974 |
| H | -2.108104 | -1.071284 | -2.040127 |
| C | -2.231505 | -3.183542 | -2.393986 |
| H | -1.532669 | -3.484951 | -1.600565 |
| H | -2.150785 | -3.919954 | -3.207108 |
| H | -3.253607 | -3.250088 | -1.992247 |
| C | -2.931392 | -1.345196 | -4.006085 |
| H | -2.743761 | -0.317336 | -4.343624 |
| H | -3.969864 | -1.411274 | -3.646647 |
| H | -2.833233 | -2.012318 | -4.876087 |
| C | 2.512812  | 0.820085  | -2.837902 |
| H | 1.956686  | 1.337168  | -2.042727 |
| C | 3.831224  | 0.313471  | -2.221712 |
| H | 3.630509  | -0.403039 | -1.414467 |
| H | 4.405295  | 1.155720  | -1.806769 |
| H | 4.466946  | -0.179513 | -2.972629 |
| C | 2.770421  | 1.841483  | -3.966526 |
| H | 1.827452  | 2.221324  | -4.383170 |
| H | 3.344751  | 1.387386  | -4.788373 |

|   |          |           |           |
|---|----------|-----------|-----------|
| H | 3.350629 | 2.695600  | -3.585083 |
| H | 0.694569 | -1.966853 | 0.000000  |

LCuOH restricted singlet, rotational minium

|    |           |           |           |
|----|-----------|-----------|-----------|
| Cu | 0.248634  | 0.018531  | 0.000000  |
| O  | -1.558305 | 0.118895  | 0.000000  |
| N  | 2.120167  | 0.014824  | 0.000000  |
| O  | 2.191171  | -3.509999 | 0.000000  |
| C  | 2.738533  | -1.171142 | 0.000000  |
| C  | 4.133248  | -1.216839 | 0.000000  |
| H  | 4.630651  | -2.186151 | 0.000000  |
| C  | 4.835019  | -0.002084 | 0.000000  |
| H  | 5.925730  | -0.008870 | 0.000000  |
| C  | 4.148228  | 1.220973  | 0.000000  |
| H  | 4.657160  | 2.184297  | 0.000000  |
| C  | 2.752830  | 1.192568  | 0.000000  |
| C  | 1.785856  | -2.344305 | 0.000000  |
| N  | 0.480485  | -1.919949 | 0.000000  |
| C  | -0.587511 | -2.858365 | 0.000000  |
| C  | -1.121992 | -3.308334 | 1.239770  |
| C  | -2.179027 | -4.228107 | 1.209421  |
| H  | -2.597162 | -4.594716 | 2.148161  |
| C  | -2.704598 | -4.687006 | 0.000000  |
| H  | -3.528054 | -5.403138 | 0.000000  |
| C  | -2.179027 | -4.228107 | -1.209421 |
| H  | -2.597162 | -4.594716 | -2.148161 |
| C  | -1.121992 | -3.308334 | -1.239770 |
| C  | -0.541852 | -2.853880 | 2.573535  |
| H  | 0.125978  | -2.004820 | 2.365966  |
| C  | 0.312773  | -3.975839 | 3.203576  |
| H  | 1.099705  | -4.310456 | 2.514455  |
| H  | -0.310275 | -4.847282 | 3.456738  |
| H  | 0.788032  | -3.621197 | 4.130938  |
| C  | -1.623839 | -2.360433 | 3.552871  |
| H  | -2.231006 | -1.559328 | 3.109150  |
| H  | -1.154779 | -1.966702 | 4.466792  |
| H  | -2.301075 | -3.172220 | 3.857308  |
| C  | -0.541852 | -2.853880 | -2.573535 |
| H  | 0.125978  | -2.004820 | -2.365966 |
| C  | 0.312773  | -3.975839 | -3.203576 |
| H  | 1.099705  | -4.310456 | -2.514455 |
| H  | 0.788032  | -3.621197 | -4.130938 |
| H  | -0.310275 | -4.847282 | -3.456738 |
| C  | -1.623839 | -2.360433 | -3.552871 |
| H  | -1.154779 | -1.966702 | -4.466792 |
| H  | -2.231006 | -1.559328 | -3.109150 |
| H  | -2.301075 | -3.172220 | -3.857308 |

|   |           |           |           |
|---|-----------|-----------|-----------|
| N | 0.505373  | 1.963058  | 0.000000  |
| O | 2.233402  | 3.536700  | 0.000000  |
| C | 1.813544  | 2.376526  | 0.000000  |
| C | -0.567707 | 2.878800  | 0.000000  |
| C | -1.107420 | 3.323273  | 1.240000  |
| C | -2.158726 | 4.246338  | 1.210483  |
| H | -2.579724 | 4.610760  | 2.149035  |
| C | -2.680345 | 4.709014  | 0.000000  |
| H | -3.501355 | 5.428177  | 0.000000  |
| C | -2.158726 | 4.246338  | -1.210483 |
| H | -2.579724 | 4.610760  | -2.149035 |
| C | -1.107420 | 3.323273  | -1.240000 |
| C | -0.550993 | 2.844828  | 2.573683  |
| H | 0.175953  | 2.048505  | 2.357575  |
| C | -1.648195 | 2.235342  | 3.468116  |
| H | -2.177097 | 1.428076  | 2.943919  |
| H | -2.390073 | 2.989294  | 3.771172  |
| H | -1.204536 | 1.822611  | 4.386768  |
| C | 0.203007  | 3.979611  | 3.299591  |
| H | 1.001849  | 4.392526  | 2.668718  |
| H | 0.654077  | 3.605698  | 4.231530  |
| H | -0.479426 | 4.801704  | 3.564028  |
| C | -0.550993 | 2.844828  | -2.573683 |
| H | 0.175953  | 2.048505  | -2.357575 |
| C | -1.648195 | 2.235342  | -3.468116 |
| H | -2.177097 | 1.428076  | -2.943919 |
| H | -1.204536 | 1.822611  | -4.386768 |
| H | -2.390073 | 2.989294  | -3.771172 |
| C | 0.203007  | 3.979611  | -3.299591 |
| H | 1.001849  | 4.392526  | -2.668718 |
| H | -0.479426 | 4.801704  | -3.564028 |
| H | 0.654077  | 3.605698  | -4.231530 |
| H | -1.915121 | -0.789350 | 0.000000  |

LCuOH triplet, rotational transition state

|    |           |           |           |
|----|-----------|-----------|-----------|
| Cu | 0.245513  | -0.326812 | 0.000000  |
| O  | 1.860045  | 0.563746  | 0.000000  |
| N  | -1.282364 | -1.561617 | 0.000000  |
| O  | -1.569904 | -1.606864 | 3.524190  |
| C  | -1.776381 | -1.981553 | 1.172271  |
| C  | -2.813248 | -2.917610 | 1.213381  |
| H  | -3.194947 | -3.238414 | 2.181827  |
| C  | -3.324428 | -3.394933 | 0.000000  |
| H  | -4.131845 | -4.128364 | 0.000000  |
| C  | -2.813248 | -2.917610 | -1.213381 |
| H  | -3.194947 | -3.238414 | -2.181827 |
| C  | -1.776381 | -1.981553 | -1.172271 |

|   |           |           |           |
|---|-----------|-----------|-----------|
| C | -1.172850 | -1.319763 | 2.386033  |
| N | -0.173876 | -0.445064 | 2.060118  |
| C | 0.366728  | 0.425739  | 3.015574  |
| C | 1.728514  | 0.242724  | 3.416296  |
| C | 2.269838  | 1.131318  | 4.347687  |
| H | 3.301195  | 1.002542  | 4.677048  |
| C | 1.509691  | 2.182374  | 4.874995  |
| H | 1.954564  | 2.865467  | 5.600609  |
| C | 0.183508  | 2.359231  | 4.472100  |
| H | -0.395212 | 3.186330  | 4.887157  |
| C | -0.413980 | 1.502267  | 3.541588  |
| C | 2.524898  | -0.947984 | 2.906328  |
| H | 2.114426  | -1.200327 | 1.918157  |
| C | 2.308511  | -2.165950 | 3.834697  |
| H | 1.241797  | -2.397499 | 3.957919  |
| H | 2.726689  | -1.971146 | 4.834303  |
| H | 2.811755  | -3.054197 | 3.423112  |
| C | 4.021334  | -0.654976 | 2.716425  |
| H | 4.173418  | 0.215913  | 2.065015  |
| H | 4.510922  | -1.519349 | 2.244241  |
| H | 4.536640  | -0.475698 | 3.672453  |
| C | -1.851036 | 1.755927  | 3.103930  |
| H | -2.101092 | 1.017898  | 2.328665  |
| C | -2.837206 | 1.555279  | 4.273143  |
| H | -2.737387 | 0.547753  | 4.697174  |
| H | -3.873203 | 1.686322  | 3.925285  |
| H | -2.659123 | 2.288227  | 5.074597  |
| C | -2.014442 | 3.152669  | 2.468145  |
| H | -3.042852 | 3.285945  | 2.100329  |
| H | -1.327690 | 3.292590  | 1.621085  |
| H | -1.816093 | 3.953188  | 3.196062  |
| N | -0.173876 | -0.445064 | -2.060118 |
| O | -1.569904 | -1.606864 | -3.524190 |
| C | -1.172850 | -1.319763 | -2.386033 |
| C | 0.366728  | 0.425739  | -3.015574 |
| C | 1.728514  | 0.242724  | -3.416296 |
| C | 2.269838  | 1.131318  | -4.347687 |
| H | 3.301195  | 1.002542  | -4.677048 |
| C | 1.509691  | 2.182374  | -4.874995 |
| H | 1.954564  | 2.865467  | -5.600609 |
| C | 0.183508  | 2.359231  | -4.472100 |
| H | -0.395212 | 3.186330  | -4.887157 |
| C | -0.413980 | 1.502267  | -3.541588 |
| C | 2.524898  | -0.947984 | -2.906328 |
| H | 2.114426  | -1.200327 | -1.918157 |
| C | 4.021334  | -0.654976 | -2.716425 |
| H | 4.173418  | 0.215913  | -2.065015 |

|   |           |           |           |
|---|-----------|-----------|-----------|
| H | 4.536640  | -0.475698 | -3.672453 |
| H | 4.510922  | -1.519349 | -2.244241 |
| C | 2.308511  | -2.165950 | -3.834697 |
| H | 1.241797  | -2.397499 | -3.957919 |
| H | 2.811755  | -3.054197 | -3.423112 |
| H | 2.726689  | -1.971146 | -4.834303 |
| C | -1.851036 | 1.755927  | -3.103930 |
| H | -2.101092 | 1.017898  | -2.328665 |
| C | -2.014442 | 3.152669  | -2.468145 |
| H | -1.327690 | 3.292590  | -1.621085 |
| H | -3.042852 | 3.285945  | -2.100329 |
| H | -1.816093 | 3.953188  | -3.196062 |
| C | -2.837206 | 1.555279  | -4.273143 |
| H | -2.737387 | 0.547753  | -4.697174 |
| H | -2.659123 | 2.288227  | -5.074597 |
| H | -3.873203 | 1.686322  | -3.925285 |
| H | 1.753246  | 1.530210  | 0.000000  |